NASA Technical Paper 1025

Validation of a Flexible Aircraft Take-Off and Landing Analysis (FATOL

Huey D. Carden and John R. McGehee

OCTOBER 1977

NASA

NASA Technical Paper 1025

Validation of a Flexible Aircraft Take-Off and Landing Analysis (FATOLA)

Huey D. Carden and John R. McGehee

Langley Research Center
Hampton, Virginia

NASA
National Aeronautics
and Space Administration

Scientific and Technical Information Office

1977

SUMMARY

Modifications to improve the analytical simulation capabilities of a multi-degree-of-freedom Flexible Aircraft Take-off and Landing Analysis (FATOLA) computer program are discussed. The FATOLA program was also used to simulate the landing behavior of a stiff-body X-24B reentry research vehicle and of a flexible-body supersonic cruise YF-12A research airplane.

The analytical results were compared with flight test data, and the correlations of vehicle motions, attitudes, axial strut forces, and accelerations during the landing impact and rollout were good. For the YF-12A airplane, airframe flexibility was found to be important for nose gear loading. Based upon the correlation study presented herein, the versatility and validity of the FATOLA program for the study of landing dynamics of aircraft are confirmed.

INTRODUCTION

Current conventional transport airplanes are subject to ground handling, structural, and control problems caused primarily by landing-gear forces and airframe interactions during taxi, take-off, and landing operations (refs. 1 and 2). These ground-induced vibration problems may be magnified for supersonic transports because of the increased structural flexibility and the higher take-off and landing speeds of these aircraft. Since landing impact and ground operations play a major role in loading the airframe, validated methods of predicting interactive characteristics of landing gear and airframe are needed to update current landing-gear design methodology and to support advanced supersonic aircraft technology.

Experimental and analytical research is being conducted by the Langley Research Center to obtain accurate predictions of ground-induced loads and vibrations and to develop active control landing-gear systems (ref. 3) which limit the loads transmitted through the gear to the airframe. To obtain improved analytical prediction of the airframe structural response, a multi-degree-of-freedom take-off and landing analysis (TOLA) computer program (refs. 4 to 7) was obtained and subsequently modified (refs. 8 and 9) to include effects of airframe flexibility on the loads and motions. The modified program called FATOLA (Flexible Aircraft Take-off and Landing Analysis) provides a comprehensive simulation of the airplane take-off and landing problem.

The purpose of this paper is to describe the modifications made to the FATOLA program to improve its simulation capabilities and to present experimental and analytical correlations of vehicle landing behavior which illustrate the capabilities of the rigid body and flexible body options and verify the analysis. Analytical simulations using FATOLA are presented for landings of two specific vehicles with passive landing gears: a stiff-body X-24B reentry vehicle and a flexible-body supersonic YF-12A research airplane. Correlations between analyti-

cal results and flight test data are made and conclusions are drawn on the validity and versatility of FATOLA.

FATOLA COMPUTER PROGRAM

Capabilities

The general capabilities of the FATOLA computer program are illustrated in figure 1. FATOLA is a modified version of the original rigid-body program (Take-off and Landing Analysis) TOLA (refs. 4 to 7). NASA Langley Research Center obtained the original program and added a flexible-body option (refs. 8 and 9) to generate the FATOLA program which has a core requirement of approximately 115K octal words on a Control Data 6600 digital computer. As indicated in figure 1, FATOLA provides a comprehensive simulation of the airplane take-off and landing dynamics. The program can represent an airplane either as a rigid body with six degrees of freedom or as a flexible body with multiple degrees of freedom. The airframe flexibility is represented by the superposition of from 1 to 20 free-free vibration modes on the rigid-body motions. The analysis has maneuver logic and five autopilots programmed to control the airplane during glide slope, flare, landing, and take-off. The program is modular so that performance of the airplane in the flight and landing phases can be studied separately or in combination.

Data which describe the vehicle geometry, flexibility characteristics, landing gear, propulsion, aerodynamic characteristics, runway roughness, and initial conditions such as attitude, attitude rates, and velocities are input to the program. A time integration of the equations of motion is performed to output comprehensive information on the airframe, state of maneuver logic, autopilots, control response, and airplane loads from impact, runway rollout, and ground operations for both the rigid-body and flexible-body options. Flexible-body and total (elastic plus rigid body) displacements, velocities, and accelerations are also obtained in the flexible body option for up to 20 points on the airplane. Complete details of the program formulation and capabilities are given in references 4 to 9.

Modifications

Subsequent to the publication of references 8 and 9, additional modifications were made at Langley Research Center to improve the analytical simulation capabilities of the FATOLA program. The modifications are discussed briefly in the following sections and details of the required program changes are presented in the appendix.

Strut axial friction.- In the original program the force in the struts attributed to axial friction was included as the component of the resultant ground force normal to the strut multiplied by a coefficient of friction applied to oppose strut motion. This formulation is incomplete (ref. 10) because the normal bearing forces depend on the moments applied to the struts. To improve the axial friction formulation, a new friction force equation was introduced to include the moment effects. In addition, a smoothing technique (ref. 11) was included to

prevent a sudden switch in magnitude and direction of the friction force at the time the strut velocity changes sign, and a change was made to allow the friction force to act before strut motion occurs as would be the case in the actual strut.

Strut air pressure equations.- A modification was made to the FATOLA program in the equations for the air pressures in the upper and lower air chambers of the strut. In the pressure equations the relationship

$$pV^{\gamma} = \text{Constant}$$

was originally programmed with the ratio of specific heats γ equal to 1.0 and where V is strut air volume and the pressure p is gage pressure. Changes were made to use absolute pressure in the pV relationship and to allow γ to take on values other than 1.0.

Structural damping.- In references 8 and 9 the dynamic motion of the airplane body is described by the normal mode method. In this method the body flexibility is represented by free-free vibration modes with no structural damping. In the flexible-body option, an equivalent viscous damping formulation (ref. 12) of structural damping was added to prevent possible analytical divergence in the flexible-body responses.

Roll autopilot and control response.- Originally, the FATOLA program logic in the roll autopilot placed the aileron deflection to a neutral setting at the time of landing impact. For an asymmetric landing of an airplane, the pilot would likely introduce aileron deflections along with pitch control in the impact and rollout phases of the landing. Changes in the roll autopilot and control response logic were therefore made to permit the simulation of variations in roll control deflections and rolling moments throughout the landing.

New input data.- These modifications to the FATOLA program require that such new input variables as strut bearing spacing, hub to lower bearing distance, atmospheric pressure, ratio of specific heats, and modal damping values be input on six data cards placed in front of the first data card of the FATOLA deck. The last three cards provide modal damping data for the flexible-body option and are always read by the program. Consequently, when the rigid-body option is being executed, these cards must also be present but may be blank.

AIRCRAFT LANDING SIMULATIONS USING FATOLA

Analytical simulations using FATOLA were conducted for the landings of two specific vehicles, a stiff-body X-24B reentry vehicle and a flexible-body supersonic cruise YF-12A research airplane.

Stiff-Body X-24B Vehicle

To verify the simulation capabilities of the rigid-body option of FATOLA, the X-24B manned lifting body research vehicle, shown in figure 2, was used. The compact delta-shaped vehicle with blended wings and flat bottom was considered to be ideal to verify the rigid-body option of FATOLA. The vehicle has been used in

a joint National Aeronautics and Space Administration and United States Air Force flight research program to explore subsonic and low supersonic flight characteristics of a manned lifting body with emphasis on the landing maneuver. During landing, the X-24B vehicle is unpowered; consequently, no thrust simulation was required.

Flight test data from an asymmetric landing of the X-24B were selected for the simulation study with FATOLA. Pertinent touchdown parameters for the unpowered landing were; sink rate, 0.49 m/s (1.6 ft/sec); ground speed, 87.1 m/s (286 ft/sec); pitch angle, 13.4°; initial pitch rate, -0.8°/s (nose over); angle of attack, 13.7°; roll angle, 2° right; and initial roll rate, 4.4°/s right roll. The X-24B had an unusual offset of 0.15 m (0.5 ft) of the center of gravity toward the right landing gear. The landing surface was assumed to be flat and smooth since the actual dry lakebed landing surface inclination and roughness were not measured. Also included in the analytical simulation were elevator (elevon) control variations to account for pilot inputs during the landing.

Flexible-Body YF-12 Airplane

The vehicle used to illustrate the capabilities of the FATOLA flexible-body option and to verify the program was the YF-12A airplane shown in figure 3. This airplane has a modified delta-wing planform and is powered by two jet engines. The fully instrumented, flexible-body supersonic research airplane was used in a NASA test program to obtain landing loads and response data (unpublished) for a flexible-body airplane.

Aircraft flexibility.- To represent the flexibility of the airplane, available modal data for an airplane in the YF-12 series were used (ref. 12). These data consist of the first 10 modal frequencies, generalized masses, deflections, and damping obtained from a two-dimensional finite-element representation of half the airplane with symmetrical boundary conditions. Consequently, the modal data are generic to the YF-12 class of airplanes only and include vertical modal deflections only. The data are limited in the spanwise direction to symmetric modes. To account for the effect of aerodynamic loading on the flexible body responses, aerodynamic weighting values were calculated, as outlined in reference 8, for the 10 flexible modes using an elliptical spanwise lift distribution over the airplane wings.

Specific flight test data for two landings, a symmetric and an asymmetric touchdown, of the YF-12A airplane were selected for simulation with FATOLA.

Symmetric touchdown.- Input touchdown parameters for the symmetric touchdown of the YF-12A airplane were: sink rate, 0.67 m/s (2.2 ft/sec); ground speed, 97.9 m/s (321 ft/sec); pitch angle, 7.2°; initial pitch rate, -0.4°/s (nose over); angle of attack, 7.65°; roll rate, 0.0°/s. Thrust data were included in the analysis to simulate the idle power of the jet engines in the landing. Programmed elevator (but no aileron) deflections were included to simulate the pilot inputs. The drag parachute deployment was also simulated. The landing surface was runway 22 at Edwards Air Force Base, California. Figure 4 presents the general runway inclination and surface roughness for approximately 1220 m (4000 ft) of the runway derived by fairing the data from a survey in which

measurements were made every 0.61 m (2 ft). The general slope and incremental surface elevations about the general slope are for a track 1.9 m (6.25 ft) (one semispan of main gear) to the right of the runway 22 center line and were input in tabular form as a function of runway distance to describe the landing surface in the analysis.

Asymmetric touchdown.- Although the available modal data for representing the airplane flexibility were limited to symmetric modes in the spanwise direction, an asymmetric touchdown was also selected for evaluation of the FATOLA program. Input touchdown parameters from the asymmetric landing were: sink rate, 0.305 m/s (1.0 ft/sec); ground speed, 84.4 m/s (277 ft/sec); pitch angle, 8.3°; initial pitch rate, -0.2°/s (nose over); angle of attack, 8.5°; roll angle, 1.2° right roll; and roll rate, 0.0°/s. As in the symmetric landing, thrust data to simulate the idle power of the jet engines were also included. Both programmed elevator and aileron control deflections were included to simulate the pilot inputs. The landing surface for this test was runway 22 at the Edwards Air Force Base, California.

RESULTS AND DISCUSSION

To demonstrate the capabilities of the rigid-body option and to verify the FATOLA analysis, results were obtained for a landing impact and rollout simulation of the stiff-body X-24B vehicle and were compared with flight test data. Verification of the flexible-body option of the program was accomplished by comparing results from two landing simulations of a flexible-body YF-12A research airplane with flight data.

Results are presented for the landing impact and rollout of the X-24B vehicle on a flat runway (actual surface undefined) and the YF-12A airplane on an inclined runway with known surface roughness as a function of runway distance. Experimental data were recorded at 200 samples/sec for both vehicles. The analytical data were generated on a Control Data 6600 series digital computer and plotted at a maximum rate of 1000 samples/sec. Data are presented from initial touchdown through nose gear contact.

Stiff-Body X-24B Vehicle

Figure 5 presents comparisons of computed and flight test time histories of elevator (upper and lower elevons) control deflections, pitch attitude, pitch rate, angle of attack; ground speed, strut strokes, and axial strut forces for the asymmetric landing impact and rollout of the X-24B vehicle. Typical computation time (using the rigid-body option of FATOLA) to generate all output data including the data in the figures was approximately 200 decimal seconds of central processing unit time with 115K octal words of storage on a Control Data 6600 series digital computer.

Elevator deflections.- Included in the FATOLA simulation were elevator (elevons on the X-24B) control variations to account for pilot inputs for pitch control during the landing. As shown in figure 5(a), the comparison of the simulated and flight test variations in the elevator deflections indicate the analy-

tical deflection rate was different from that of the flight test data; however, because of the overall good agreement of the data presented in figures 5(b) to 5(d), no attempt was made to match the control rate more closely. As noted in figure 5(a), at a time of 2.2 sec the lift coefficient for the X-24B was analytically staged to a value which reflected the effect of the lower elevons being experimentally deflected down to approximately 16°. The best available ground effect aerodynamics on the vehicle did not include aileron effectiveness; therefore, aileron variations were not simulated.

Pitch attitude.- In figure 5(b) the predicted pitch attitude is in excellent agreement with the flight test data to approximately 1.7 sec and agrees well for the remainder of the time history. For the X-24B on a level runway, the static strut strokes and vehicle geometry result in an indicated negative pitch angle of approximately 2°.

Pitch rate.- Figure 5(c) presents a comparison of the analytical and experimental time histories of pitch rates for the X-24B. Nose-over pitch rates are negative and zero time corresponds to touchdown. The data are plotted to a time beyond nose gear impact which occurred at approximately 1.7 sec.

The figure indicates a slight time shift of about 0.2 sec between the computed and actual time histories that may be attributed to the influence of the actual landing surface which was not available for input. Magnitudes and trends of the computed and experimental pitch rates, however, are in good agreement throughout the time history.

Angle of attack.- A comparison of the computed and experimental angle of attack in figure 5(d) indicates good agreement although the analytical values are slightly higher than flight test data throughout the time history. The maximum deviation between the computed and experimental angles is approximately 2° but generally the deviation is less than 1°.

Ground speed.- A comparison of the experimental and computed ground speed is presented in figure 5(e). Good correlation is shown throughout the time history although the analytical ground speed is slightly higher beyond approximately 1.5 sec. The higher speed is consistent with the assumed flat and smooth landing surface as opposed to the actual surface which likely had both inclination and surface roughness which could affect ground speed.

Strut strokes.- In figures 5(f), 5(g), and 5(h), analytical and experimental time histories of strut stroke for the right main, left main, and nose gear, respectively, are compared for the X-24B vehicle landing. The overall agreement between the magnitude and trends of the computed strut strokes and the flight test data are excellent for the right main (fig. 5(f)) and nose gear (fig. 5(h)) although the computed nose gear stroke is slightly higher on the second peak around 3.0 sec. In figure 5(g), however, the results for the left gear show differences in the initial stroke but overall behavior and maximum strokes are in good agreement. As was the case with the flight data, the computed left strut stroke is less than that of the right main gear because of the offset of the center of gravity toward the right gear.

Axial strut forces.- Flight test axial strut forces and computed results for the X-24B are compared in figures 5(i) to 5(k). In figure 5(i), the comparison of axial strut force indicates that the overall shape of the time history, the time of occurrence of the peak forces, and, in general, the magnitudes of the experimental and analytical results are in good agreement for the right main gear. An overprediction of the force at 1.1 sec can be attributed to an additional analytical stroke (in excess of the experimental) of 0.014 m (0.045 ft) of the strut at 1.1 sec. (See fig. 5(f).) Such results indicate the sensitivity of forces to the pneumatic component of the axial strut force during low or essentially zero strut compressive velocities. Beyond approximately 2.4 sec, the analytical main gear forces have leveled off whereas the flight data for both the right and left gears are oscillatory probably from the dry lakebed roughness which was not modeled in the analysis.

As indicated in figure 5(j), the agreement between the computed left gear force and flight data are not as good as the right gear comparison. The analytical forces are lower at initial contact and beyond 1.5 sec in the time history. However, the analytical results do appear to be more rational than the experimental data. For example, the left gear stroke, both experimentally and analytically, was less than the right gear stroke during the rollout phase. (See figs. 5(g) and 5(h).) At a constant stroke the vehicle is supported primarily by the force of the compressed air volume in the struts. It is expected that experimental forces in the gear with the smaller stroke would be less than those in the gear with the larger stroke. A comparison of the gear forces in figures 5(i) and 5(j), however, indicates that the experimental left gear forces are the same level or slightly higher than those of the right gear which is stroked more. This apparent discrepancy is not understood.

In figure 5(k), the computed nose gear force shows a more rapid onset in loading but the peak force is in excellent agreement with flight data and the strut forces are only slightly higher throughout the remainder of the time history which is consistent with the strut stroke data (fig. 5(h)). The overall good agreement of the comparisons between the experimental and computed results for the X-24B vehicle indicate that the rigid-body option of FATOLA is a valid tool for the study of landing dynamics of stiff-body vehicles.

Flexible-Body YF-12A Airplane - Symmetric Touchdown

Figure 6 presents a comparison of flight test and analytical time histories of elevator deflections, pitch attitude, pitch rate, angle of attack, ground speed, strut strokes, axial strut forces, drag parachute force, longitudinal acceleration, and normal body accelerations, for a symmetric touchdown of the YF-12A research airplane. With the flexible-body option of FATOLA, typical computation time for generating all output data including the data of figure 6 was approximately 2400 decimal seconds of central processing unit time with 115K octal words of storage on a Control Data 6600 series digital computer.

Elevator deflections.- The elevator variations executed by the pilot to control the nose gear impact and the analytical simulation are shown in figure 6(a). The analytical variations of elevator deflections were programmed as shown to

follow the actual flight test variations (computed from the two inboard and two outboard elevons on the airplane) throughout the time history.

During the analytical study, pitch rate was found to be extremely sensitive to the aerodynamic derivative $C_{m_{\delta q}}$ which expresses the rate of change of the pitching-moment coefficient with elevator deflections; hence, slight reduction in the aerodynamic derivative was made (≈10 percent) to obtain the correlation with flight data. Since the aerodynamic data used were derived from wind-tunnel tests on a 1/12-scale rigid model, the reduced aerodynamic coefficient is consistent with references 13 and 14 which indicate that airframe flexibility reduces the elevator effectiveness of a real airplane below that of a rigid airplane.

Pitch attitude.- A comparison of the experimental and analytical pitch attitude is presented in figure 6(b) for the symmetric landing impact and rollout of the YF-12A airplane. Although the analytical results are slightly higher beyond 3 sec, they are within 1° or less of the flight data throughout the time history.

Pitch rate.- Presented in figure 6(c) is a comparison of the analytical and actual time histories of the YF-12A airplane pitch rate response. The general variations in the magnitude of the pitch rate reflect the influence of approximately 22 changes in the aerodynamic control inputs (fig. 6(a)) executed by the pilot to reduce the nose gear impact at approximately 12.0 sec. The higher frequency oscillations in the flight data are responses of the pitch rate sensor to structural inputs.

As indicated in the figure, the magnitude and trends of the analytical and flight test time histories are in good agreement throughout the 15 sec of the landing impact and rollout. However, between approximately 13 and 13.5 sec, the flight data indicate a reduction in nose-over pitch rate that is not evident in the analytical results. A drift of the airplane approximately 4.6 m (15 ft) to the right of the runway center line placed the airplane on a track which may have had different surface roughness from that simulated (fig. 4) in the analysis and may have been responsible for this variation.

Angle of attack.- The comparison, in figure 6(d), between the flight test and analytical angles of attack are similar in behavior to the pitch attitude (fig. 6(d)) as would be expected. The magnitude of the analytical data is within 1° or less of the flight data throughout the time history. At nose gear impact, the flight data become erratic and are not plotted beyond that time.

Ground speed.- In figure 6(e) the comparison between the computed and experimental ground speed of the YF-12A for the symmetric touchdown and rollout indicates excellent agreement throughout the 15.0-sec time history presented. During this time the airplane traversed approximately 1189 m (3900 ft) of runway 22 at the Edwards Air Force Base. (See fig. 4.) The effect of drag parachute deployment is evident in the sharp decrease in ground speed beyond 6.0 sec. At the end of 15 sec the computed speed is only approximately 2 percent lower than the experimental speed.

Strut strokes.- Shown in figures 6(f), 6(g), and 6(h) are the experimental and analytical strut strokes of the right and left main gears, and nose gear,

respectively, for the symmetric landing of the YF-12A. As indicated in figures 6(f) and 6(g), there is generally good agreement between the flight data and analytical results. In both cases there was minimum stroking of the gears during approximately the first 8.0 sec of touchdown and rollout. Some differences between the experimental and analytical strokes were evident. For example, between approximately 1.5 and 3.0 sec, one stroke pulse was indicated in the analytical results and a series of four small stroke pulses was indicated in the flight data. Although the exact cause of such differences was not established, deviations in the runway roughness or slight variations in pitch rate (fig. 6(c)) could produce significant changes in stroke behavior.

Major stroking of the main gears, both experimentally and analytically, occurred beyond 8.0 sec in the rollout. The trends compared well and the maximum analytical strokes were only approximately 10 to 12 percent higher beyond 12.0 sec.

In figure 6(h) the comparison of experimental and analytical nose gear strokes is not as good as the comparisons for the main gears. Although the times of nose gear contact are the same, the initial peak analytical stroke was less than the experimental stroke. For subsequent stroking, the flight data had three small stroke pulses between 12.5 and 15 sec whereas the analytical had a substantial second peak in stroke with a smaller third pulse. This difference in nose gear strokes could have resulted from the nose gear encountering a different runway roughness than was input because of the drift of the airplane across the runway.

Axial strut forces.- Comparisons of the experimental and analytical right and left main gear and nose gear axial strut forces are presented in figures 6(i), 6(j), and 6(k), respectively. In figures 6(i) and 6(j) the main gear axial strut forces show excellent correlation in magnitude and pattern throughout the time history. Between 5.5 and 6.5 sec both the experimental and analytical force levels decreased; however, the analytical results indicated the tires briefly lost contact with the runway.

In figure 6(k) the correlation of the experimental and analytical nose gear axial strut forces was not as good as the main gear force comparisons. The trends of the nose gear axial strut forces are, however, consistent with the nose gear strokes and pitch rate behavior because of their interrelationship. Consequently, the differences noted in figure 6(k) are also attributed to possible differences in runway roughness discussed previously.

Drag parachute force.- During the symmetric touchdown of the YF-12A airplane, the pilot deployed the drag parachute of the airplane approximately 6 sec after initial main gear contact. Figure 6(l) presents a comparison of the experimental and analytical drag parachute force time histories. The comparison indicates excellent correlation in magnitude and decay of the parachute forces from initial deployment. The agreement shown in the figure is also consistent with the excellent correlation of ground speed of the airplane (fig. 4(e)).

Longitudinal body accelerations.- Figure 6(m) shows the comparison between the experimental and analytical longitudinal acceleration of the center of gravity of the YF-12A airplane. Excellent correlation is shown between the magni-

tudes and variations of the computed and flight data accelerations. Although some high frequency response is present on the flight data, the primary response of the longitudinal acceleration is a rigid-body response and reflects the effects of various drag forces acting on the airplane in the longitudinal direction. For example, the sudden change in acceleration to approximately -0.55g shortly after 6 sec is the effect of the drag parachute deployed at that time. (1g = 9.8 m/sec^2 or 32 ft/sec^2.) As the speed of the airplane decreases (along with the drag parachute force, fig. 6(e)), the acceleration slowly increases to less negative values throughout the remainder of the time history.

Normal body accelerations.- Comparisons of flight test and analytical normal accelerations at the center of gravity, the cockpit, and left main gear-body interface on the YF-12A airplane are shown in figures 6(n), 6(o), and 6(p), respectively. Although differences are evident in the figures, there are important points of similarity to be noted. For instance, in figure 6(n) the flight data accelerations, shown on an expanded time scale in the insert sketch, indicate that the first and ninth experimental modes at 3.4 Hz and 23 Hz, respectively (refs. 15 and 16), were the predominant modes contributing to the acceleration responses of the airplane. Similarly, the analytical responses at 2.5 Hz and 18 Hz were the first and ninth analytical symmetric modes of the 10 two-dimensional modes used to represent the flexibility of the airplane.

Figure 6(o) presents a comparison of experimental and analytical accelerations at the cockpit. Accelerations experienced by the pilot can affect his capability to control the airplane and monitor the cockpit instruments during take-off and landing. As indicated in the figure, the predominant modes contributing to the experimental acceleration response were the first and seventh symmetric modes at 3.4 Hz and 12 Hz, respectively. Likewise, the analytical responses were the first and seventh analytical modes at 2.5 Hz and 14.5 Hz, respectively. At the time of nose gear impact, the agreement between the analytical and flight data is good. The differences between the analytical and flight test amplitudes could be attributed, in part, to apparently higher analytical modal damping than that exhibited on the aircraft (compare the decay of oscillations) and to differences between the analytical and experimental modes (that is, dissimilar nodal locations, modal amplitudes, and frequencies). Since similar modes are being excited in both the analysis and the flight test of the YF-12A airplane, the use of more accurate modes and frequencies would likely improve the acceleration correlations.

In figure 6(p) only a segment of the flight test acceleration at the left main gear-body interface is presented for comparison of predominant response frequencies with the analytical results since the flight data had a zero shift. The comparison indicates that the predominant modes contributing to both the experimental and analytical acceleration responses were the first and ninth symmetric modes, however, at the different modal frequencies previously discussed. Since this landing impact was symmetric, it would be unlikely that any significant asymmetric responses would be present in the spanwise direction on the airplane. The data presented in figure 6 indicate that the FATOLA program can adequately predict the significant loads and responses for a flexible-body airplane during a symmetric touchdown.

Flexible-Body YF-12A Airplane - Asymmetric Touchdown

As indicated in a previous section, the available modal data used to represent the airplane flexibility were limited to symmetric modes in the spanwise direction. However, an asymmetric touchdown of the YF-12A was selected for evaluation of FATOLA.

Figure 7 presents comparisons of analytical and flight test time histories of elevator and aileron control deflections, pitch attitude, pitch rate, roll rate, angle of attack, ground speed, strut strokes, axial strut forces, and normal body accelerations for the asymmetric landing impact and rollout of the YF-12A research airplane. The data of figure 7 were obtained with the flexible-body option of FATOLA in approximately 1800 decimal seconds of central processing unit time with 115K octal words of storage on a Control Data 6600 series digital computer.

Elevator deflections.- Elevator control deflections and the analytical programmed variations are shown in figure 7(a). The sensitivity of the pitching-moment coefficient with elevator deflections noted in the symmetric touchdown also required a reduction of ≈10 percent of the available aerodynamic coefficient on elevator deflections to achieve good correlation with flight data during this asymmetric simulation.

Aileron deflections.- Since the YF-12A airplane had a roll angle of 1.2° to the right at touchdown, considerable aileron control deflections were initiated by the pilot during the asymmetric landing for roll control. Figure 7(b) presents the experimental aileron deflection and the analytical inputs of the aileron control.

Pitch attitude.- A comparison of the experimental and analytical pitch attitude time histories are presented in figure 7(c) for the asymmetric impact and rollout of the YF-12A airplane. Good agreement is shown between the analytical results and the flight test data to beyond nose gear impact which occurred at approximately 6.5 sec.

Pitch rate.- Presented in figure 7(d) is a comparison of the computed and flight test time histories of the pitch rate response for the YF-12A airplane. The figure indicates that the magnitudes and trends of the analytical and flight test time histories are in good agreement throughout the initial 10 sec of the asymmetric landing and rollout. The general variations in the pitch rate reflect the pilot's use of the elevators to control the pitch rate prior to nose gear impact whereas the higher frequencies are responses of the pitch rate sensor to structural inputs noted previously.

Roll rate.- A comparison of the experimental and analytical roll rate of the YF-12A airplane is presented in figure 7(e). The data indicate that the correlation between experimental and analytical roll rate is good during the initial phase of the impact. Beyond approximately 2 sec, the oscillations of roll rate are out of phase with the experimental data but the peak values agree well. The differences in phase of analytical results may be attributed to the absence of antisymmetric modes in the flexibility representation in the spanwise direction.

Angle of attack.- Comparisons between the flight data and analytical angle of attack are presented in figure 7(f). The analytical angle of attack shows a smooth decrease as the airplane pitches over during the landing as would be expected. The experimental data, however, are erratic and are suspect especially beyond approximately 3.0 sec.

Ground speed.- During the first 10.0 sec of the asymmetric touchdown and rollout, the airplane traversed approximately 792 m (2600 ft) of runway 22 at the Edwards Air Force Base. (See fig. 4.) In figure 7(g) the comparison of the computed and experimental ground speed indicates good agreement throughout the time history. Since the drag parachute was not deployed during this part of the rollout, the decrease of the airplane ground speed is the result of all other drag forces opposing the forward motion of the airplane.

Strut strokes.- A comparison between the analytical and experimental main gear and nose gear strut strokes could not be made because of a loss of the strut stroke data channels for this particular flight. However, figure 7(h) presents the analytical strokes for completeness of data presentation. The data indicate that the main gear strut strokes, in the latter part of the time histories, were oscillating slightly about a level of approximately 0.26 m (0.85 ft). The nose gear strut stroke was still transient during the time history presented.

Axial strut forces.- Comparisons of the experimental and analytical axial strut forces which resulted during the asymmetric landing impact and rollout of the YF-12A airplane are presented in figures 7(i) to 7(k). As indicated in the figures, the overall shapes and magnitudes of all three analytical axial-force time histories agree well with the flight data time histories. At approximately 3.3 sec, however, and from 7.5 to 10.0 sec, the analytical right main axial strut forces (fig. 7(i)) were somewhat higher than the flight data. In figure 7(j), the left main gear force was lower at approximately 3.5 sec. Oscillations of the analytical forces in the main gears are out of phase with the flight data in the latter stage of the time histories.

Differences in the magnitude and phasing of the analytical and flight data time histories (for both right and left main gears) might be attributed to the absence of spanwise antisymmetric modes. If antisymmetric degrees of freedom had been included in the analysis, it is believed that the overprediction of the right gear and the underprediction of the left gear strut forces would both have been substantially reduced.

In figure 7(k) the analytical and experimental nose gear axial strut force time histories are in very good agreement. Since the nose gear is on the vehicle plane of symmetry, the antisymmetric spanwise motions would not be expected to appreciably affect the results for the nose gear. For this landing, the airplane remained close to the measured track of runway roughness and better agreement between the nose gear axial forces was indicated as compared with the symmetric touchdown discussed previously.

Normal body accelerations.- Comparisons of flight test and analytical normal accelerations at the center of gravity, cockpit, and left main gear-body interface are shown in figures 7(l), 7(m), and 7(n), respectively, for the asymmetric landing of the YF-12A airplane. In figures 7(l) and 7(m), the same important

points of similarity noted in the symmetric touchdown (figs. 6(n) to 6(p)) are also evident in these comparisons. For instance, in figure 7(l) at the center of gravity, both the flight test and analytical acceleration response frequencies (experimentally at 3.4 Hz and 23 Hz and analytically at 2.5 Hz and 18 Hz, respectively) which correspond to the first and ninth symmetric modes are the predominant contributions to the responses.

At the cockpit (fig. 7(m)), the predominant experimental acceleration response frequencies correspond to the first mode (3.4 Hz) and the eight symmetric mode (15 Hz). For the analytical accelerations, the predominant responses were the first and ninth analytical modes. Since the center of gravity and cockpit positions are in the plane of symmetry of the airplane, the asymmetric landing and the absence of antisymmetric spanwise modes would not be expected to appreciably affect the results for these vehicle locations. On the other hand, possible differences between the flight test and analytical responses could be expected for the left main gear and body interface comparison shown in figure 7(n). Indeed, the analytical results indicate that the predominant response frequencies of 2.5 Hz and 18.0 Hz correspond to the first and ninth symmetric modes whereas the experimental response frequencies of 4.3 Hz and 29.0 Hz correspond to the first and sixth experimental antisymmetric modes of the airplane.

The comparisons of the experimental and analytical data for the asymmetric touchdown of the YF-12A airplane indicate that the FATOLA program can adequately describe the significant airplane loads and responses. The use of more accurate modal data including antisymmetric modes should improve significantly the acceleration correlations for an asymmetric touchdown case.

Flexibility Effects

An important effect that the available flexibility data have in altering the loading behavior on the YF-12A airplane is shown by the comparison in figure 8 of the analytical rigid-body and flexible-body nose gear axial strut forces. The rigid-body data indicate three nearly complete unloadings with six major peaks between 6.5 and 10 sec in the time history. The introduction of symmetric flexibility significantly altered the load pattern to only one complete unloading and four major peaks with slightly higher magnitude of forces than the rigid-body forces. For the flexible-body option, the nose gear contact occurred approximately 0.3 sec later than the rigid-body option results. As indicated in figure 7(k), both the magnitudes and load pattern of the flexible data are in good agreement with the experimental force behavior. These results indicate that airframe flexibility can be important in load prediction. The rigid-body data in figure 8 were from a computer run which required 600 decimal seconds of central processing unit time with 115K octal words of storage on a Control Data 6600 series digital computer.

CONCLUDING REMARKS

A Flexible Aircraft Take-off and Landing Analysis computer program (FATOLA) is used in an experimental and analytical correlation study of vehicle landing behavior to demonstrate the rigid-body and flexible-body options of the program

and to validate the analysis. Modifications to the program to improve the analytical simulation capabilities of the FATOLA program are discussed.

Based on correlations between analytical and experimental data for both the X-24B vehicle and the YF-12A airplane, overall agreement between the analytical and flight test data is good. For the YF-12A airplane, airframe flexibility is important for nose gear loading. Differences are evident between analytical acceleration magnitudes and flight data for the YF-12A; however, similar modes appear in the analytical results and the flight data. The use of more accurate symmetric and antisymmetric modes and frequencies would likely improve the acceleration correlations. The present correlations indicate, however, that the FATOLA program is a versatile and valid analytical tool for the study of aircraft landing dynamics.

Langley Research Center
National Aeronautics and Space Administration
Hampton, VA 23665
September 7, 1977

APPENDIX

PROGRAMMING CHANGES

This appendix presents the changes in the FATOLA program to improve the analytical simulation capabilities.

Strut Axial Friction

Three modifications were made to improve the strut axial friction force simulation. To accomplish the first two modifications, the following statements were inserted in the LGEA3C subroutine of FATOLA:

```
      COMMON/NORMFF/SLEN1(5), SLEN2(5)
      COMMON/TEMPRES/GAMA, PATM
      DIMENSION IFRI (5)
      DATA (IFRI(I), I = 1,5)/0,0,0,0,0/
      IF(SD1(1,I).EQ.0.0.AND.IFRI(I).EQ.1)IFRI(I)=0
      IF(SD1(1,I).LE.0.5.AND.IFRI(I).EQ.0)2,3
    2 HYPTAN = 1.0
      GO TO 4
    3 HYPTAN = ABS (TANH(4.0*SD1(1,I)))
      IFRI(I) = 1
    4 FF(I) = MUS(I)*SQRT(FDX(I)*FDX(I)+FDY(I)*FDY(I))
      FF(I) = FF(I)*(1.0+2.0*((SLEN2(I)-S(1,I))/
              (SLEN1(I)+S(1,I))))*HYPTAN
```

The two COMMON statements allow the new input variables to be passed into subroutine LGEA3C. The DIMENSION statement sizes the friction indicators IFRI(I), and the DATA statement initializes the indicators to zero. The two IF statements and HYPTAN = 1.0 allow the full friction force to be used until the strut velocity SD1(1,I) of any strut drops below 0.152 m/s (0.5 ft/sec) (arbitrarily chosen) after the initial stroking. When the strut velocity becomes less than 0.152 m/s (0.5 ft/sec), the friction force is transitioned through zero along the hyperbolic tangent function

```
HYPTAN = ABS (TANH (4.0*SD1(1,I))).
```

The original strut axial friction force equation (statement numbered 4) was modified to a form of equation (4) in reference 10 to include the moment effects on the axial friction. The expression is

```
FF(I) = FF(I)*(1.0+2.0*((SLEN2(I)-S(1,I))/(SLEN1(I)+S(1,I))))
```

where

SLEN2(I) array of distances between hub and lower bearing for fully extended gear

SLEN1(I) array of distances between upper and lower bearing for fully extended gear

S(1,I) strut strokes for each gear

The third modification was to change the statement

```
TMP(2) = 0.0
```

in the subroutine LGEAR1 to

```
TMP(2) = 1.0
```

which allows the friction force to be effective at all times.

Strut Air Pressure Equations

Revised strut air pressure equations were also inserted in the LGEA3C subroutine to replace the original equations. The revised equations are

```
P (I) = (PZERO(I)+PATM)*(VZERO(I)/(VZERO(I)+A2(I)*S2(1,I)-S(1,I)*A(I)))**GAMA-PATM

P2(I) = (P20(I)+PATM)*(V20(I)/TMP(1))**GAMA-PATM
```

where PATM (atmospheric pressure) has been included to convert gage pressure to absolute pressure and GAMA (γ) has been added to allow variations in the compression process.

Structural Damping

To incorporate structural damping in the flexible body simulation, the statement

```
COMMON/DAMPCOM/GDAMP(20)
```

and expression

```
GTF(IG)=GQ(IG)*GMASS1(IG)*GFREQ(IG)**2+GQD1(IG)*GDAMP(IG)
```

were added to the subroutine FLEX1 of the FATOLA program. The COMMON statement makes available the necessary input variable GDAMP (modal damping) in the FLEX 1 subroutine. The second term of the expression

```
GQD1(IG)*GDAMP(IG)
```

represents the modal damping force that has been added. As stated in reference 12, the equivalent viscous form of structural damping GDAMP(IG) can be approximated by

$$GDAMP(IG) = K_{jj}\, g_j/\omega_j$$

where

K_{jj} jth generalized modal stiffness

g_j structural damping in jth mode (usually based on experimental data)

ω_j jth vibration natural frequency

Roll Autopilot and Control Response

To permit variations in roll control deflections to be simulated throughout the landing, the logic in the roll autopilot and control response sections were altered in the auxiliary computations routine of the program. For the roll autopilot the changes were

```
102 IF(IAP.EQ.4) GO TO 68
    DELPD=0
    GO TO 103
 68 IF(TR.LE.TST) GO TO 69
    DELPDE = DELPI+DELA*(TR-TST)
    GO TO 103
 69 DELPI = DELPD
    GO TO 103
```

and in the control response

```
 63 IF(IAP.EQ.4) GO TO 64
```

The changes given create, in the roll autopilot, a special branch for the landing impact and rollout phase (IAP = 4) to allow the aileron deflections to be initialized and programmed by inputs of DELPD (initial input aileron deflection), TST (time for staging), and DELA (aileron rate). The addition of statement 63 in the control response also switches the logic only for IAP = 4 to set the actual aileron deflection, used elsewhere in the program, to the desired value of aileron deflection (DELPDE) computed in the roll autopilot.

New Input Data

To make the new variables associated with the modifications to FATOLA available to the program subroutine where they are used, the programming changes presented below were added to the main program TOLA.

```
     COMMON/NORMFF/SLEN1(5),SLEN2(5)
     COMMON/TEMPRES/GAMA,PATM
     COMMON/DAMPCOM/GDAMP(20)
     NAMELIST/BEGDATA/SLEN1,SLEN2,GAMA,PATM,GDAMP
     READ(5,5002)SLEN1,SLEN2
5002 FORMAT(5F10.0)
     READ(5.5003)GAMA, PATM
5003 FORMAT(2F10.0)
```

```
      READ(5.5004)GDAMP
5004  FORMAT(8F10.0)
      WRITE(6,BEGDATA)
```

The common statements establish labeled common blocks for the variables in NAMELIST. The READ and FORMAT statements initiate the reading of the new data cards. The WRITE statement initiates printing of the new input data list prior to the read and print of the normally specified FATOLA input data.

REFERENCES

1. DC-10 Landing Gear Modified. Aviat. Week & Space Technol., vol. 98, no. 12, Mar. 19, 1973, p. 181.

2. Ropelewski, Robert R.: Airbus Test Tempo Quickening. Aviat. Week & Space Technol., vol. 98, no. 10, Mar. 5, 1973, pp. 32-35.

3. McGehee, John R.; and Carden, Huey D.: A Mathematical Model of an Active Control Landing Gear for Load Control During Impact and Roll-Out. NASA TN D-8080, 1976.

4. Lynch, Urban H. D.: Takeoff and Landing Analysis (TOLA) Computer Program. Part I - Capabilities of the Takeoff and Landing Analysis Computer Program. AFFDL-TR-71-155, Pt. 1, U.S. Air Force, Feb. 1972. (Available from DDC as AD 741 942.)

5. Lynch, Urban H. D.; and Dueweke, John J.: Takeoff and Landing Analysis (TOLA) Computer Program. Part II.- Problem Formulation. AFFDL-TR-71-155, Part II, U.S. Air Force, May 1974.

6. Lynch, Urban H. D.; and Dueweke, John J.: Takeoff and Landing Analysis Computer Program (TOLA). Part III.- User's Manual. AFFDL-TR-71-155, Part III, U.S. Air Force, Apr. 1974.

7. Young, Fay O.; and Dueweke, John J.: Takeoff and Landing Analysis Computer Program (TOLA). Part IV: Programmer's Manual. AFFDL-TR-71-155, Part IV, U.S. Air Force, Jan. 1975.

8. Dick, J. W.; and Benda, B. J.: Addition of Flexible Body Option to the TOLA Computer Program. Part I - Final Report. NASA CR-132732-1, 1975.

9. Dick, J. W.; and Benda, B. J.: Addition of Flexible Body Option to the TOLA Computer Program. Part II - User and Programmer Documentation. NASA CR-132732-2, 1975.

10. Milwitzky, Benjamin; and Cook, Francis E.: Analysis of Landing-Gear Behavior. NACA Rep. 1154, 1953. (Supersedes NACA TN 2755.)

11. Wignot, Jack E.; Durup, Paul C.; and Gamon, Max A.: Design Formulation and Analysis of an Active Landing Gear. Volume I. Analysis. AFFDL-TR-71-80, Vol. I, U.S. Air Force, Aug. 1971. (Available from DDC as AD 887 127L.)

12. Edinger, Lester D.; Schenk, Frederick L.; and Curtis, Alan R.: Study of Load Alleviation and Mode Suppression (LAMS) on the YF-12A Airplane. NASA CR-2158, 1972.

13. Fung, Y. C.: An Introduction to the Theory of Aeroelasticity. GALCIT Aeronautical Series. John Wiley & Sons, Inc., c.1955.

14. Etkin, Bernard: Dynamics of Flight. John Wiley & Sons, Inc., c.1959.

15. Kordes, E. E.; and Curtis, A. R.: Results of NASTRAN Modal Analyses and Ground Vibration Tests on the YF-12A Airplane. Paper 75-WA/Aero 8, Amer. Soc. Mech. Eng. Winter Annual Meeting (Houston, Texas), Nov.-Dec. 1975.

16. Wilson, Ronald J.; Cazier, Frank W., Jr.; and Larson, Richard R.: Results of Ground Vibration Tests on a YF-12 Airplane. NASA TM X-2880, 1973.

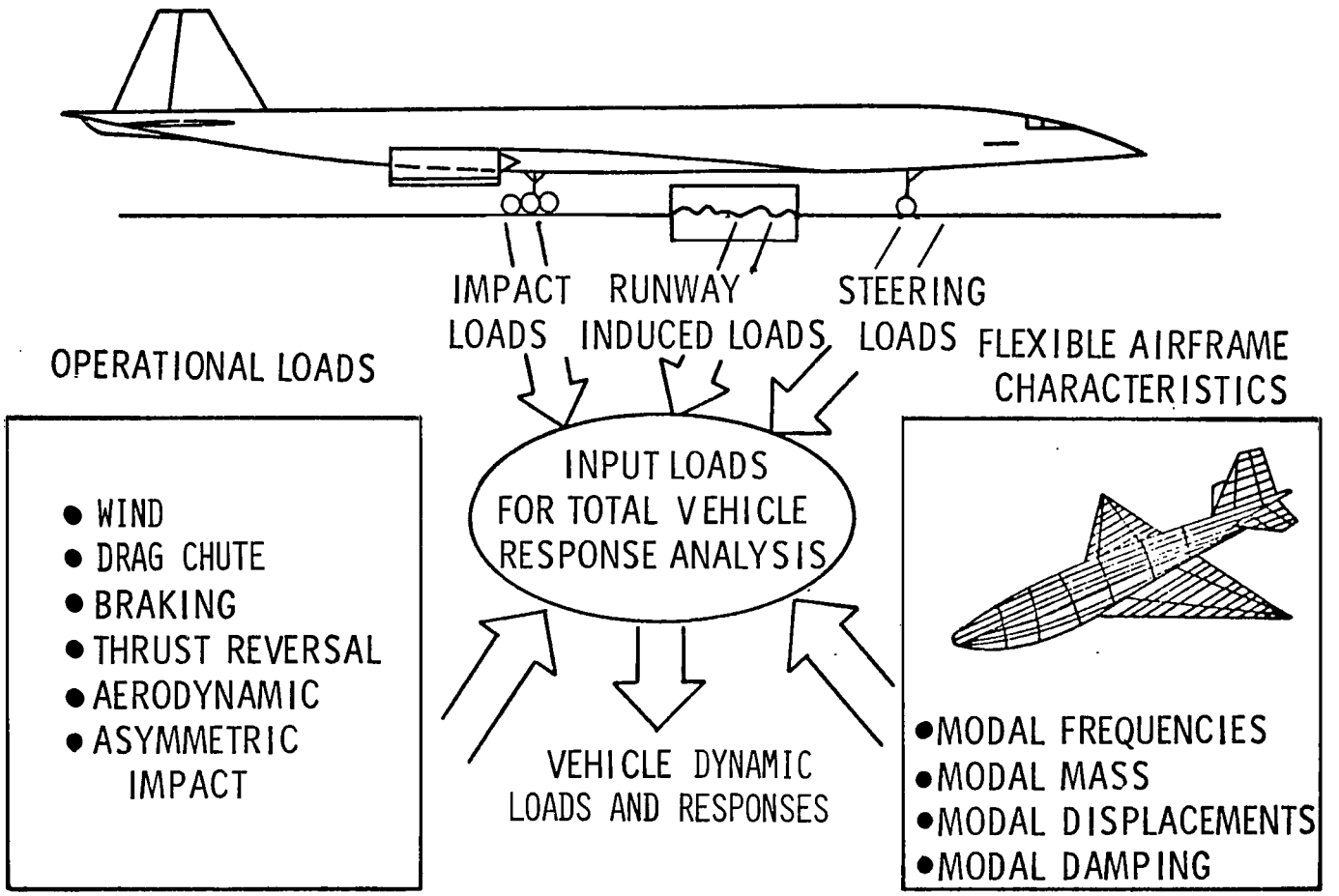

Figure 1.- General capabilities of the Flexible Aircraft Take-off and Landing Analysis (FATOLA) computer program.

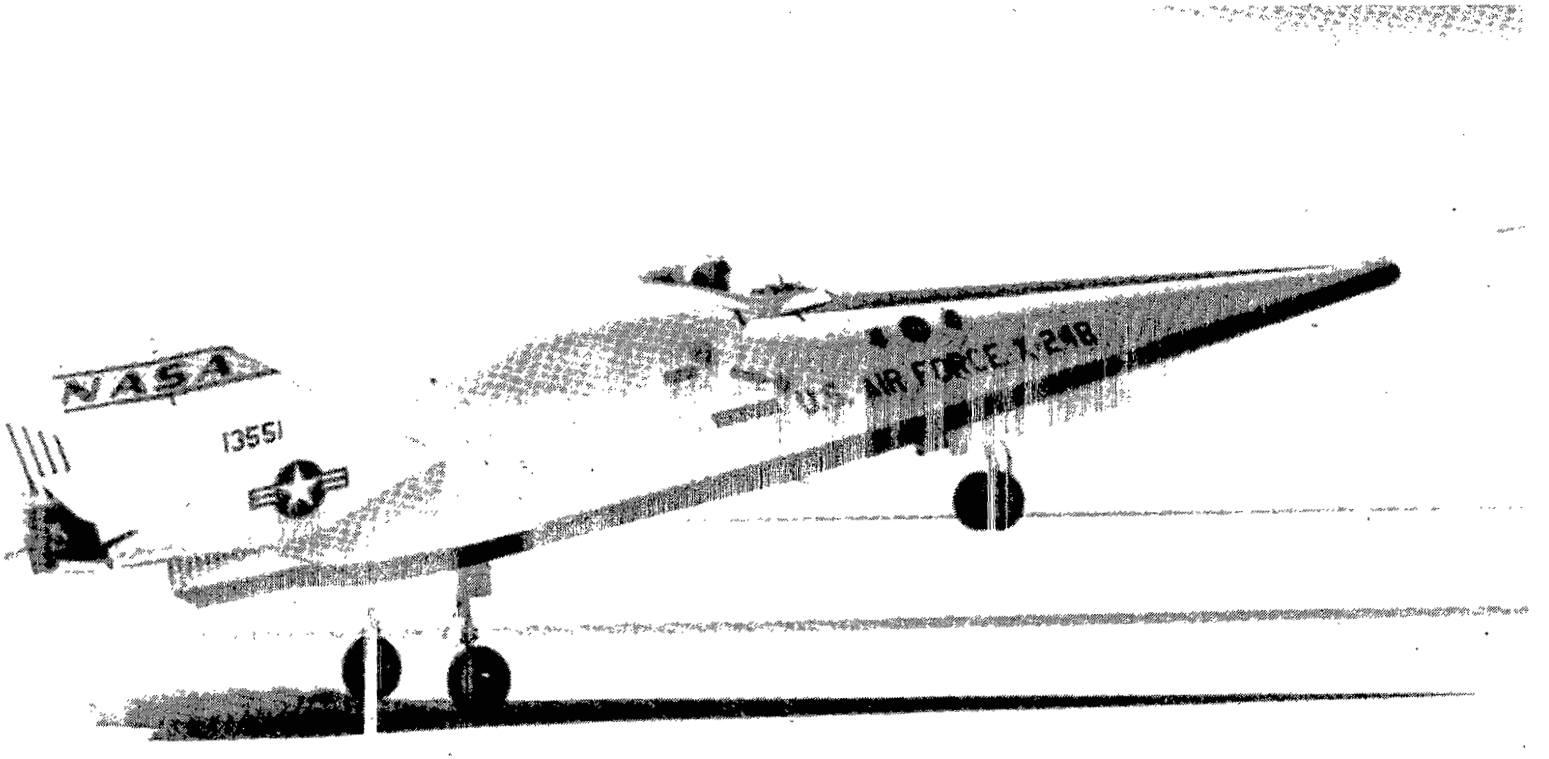

L-77-278

Figure 2.- X-24B reentry research vehicle.

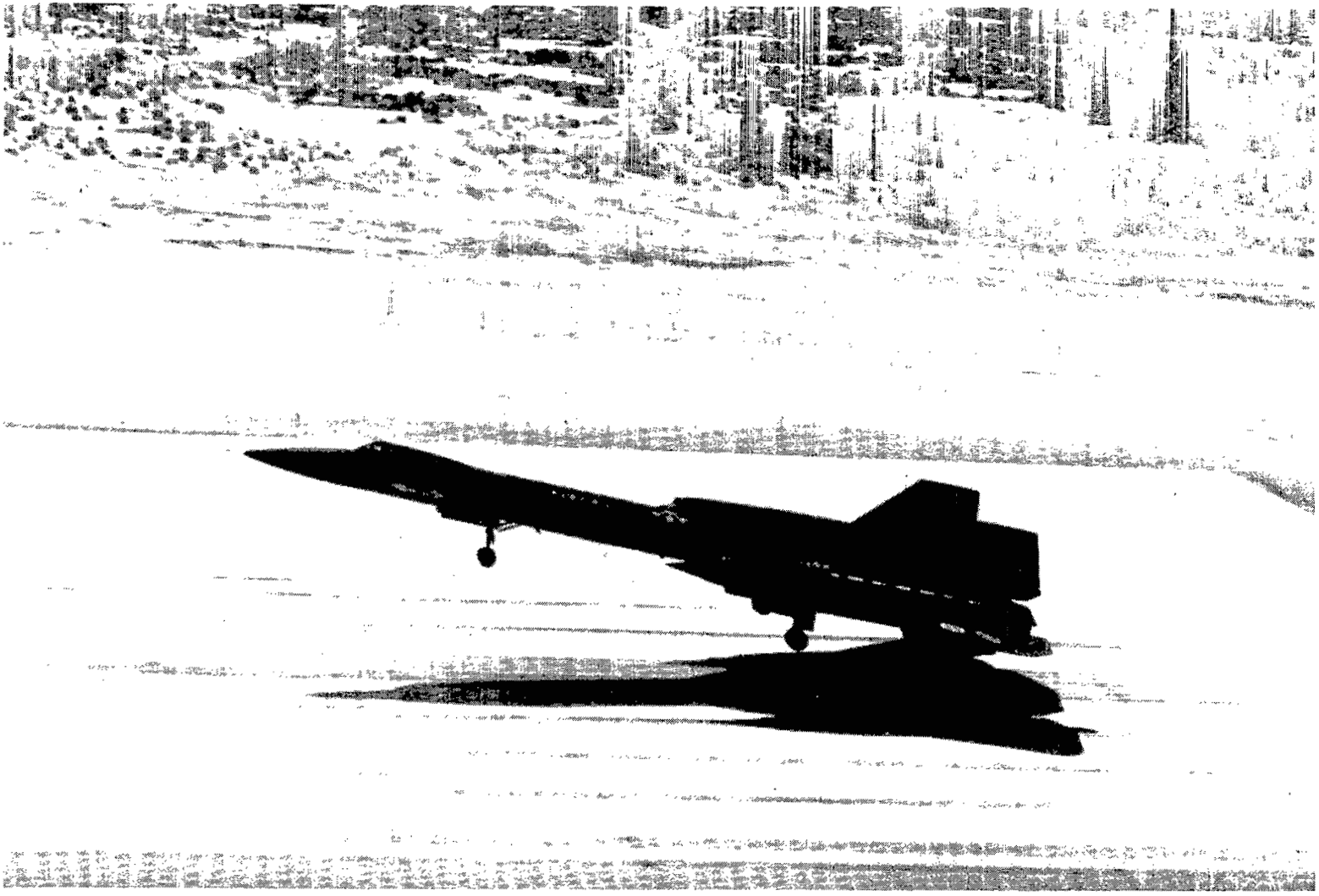

L-77-279

Figure 3.- YF-12A research airplane.

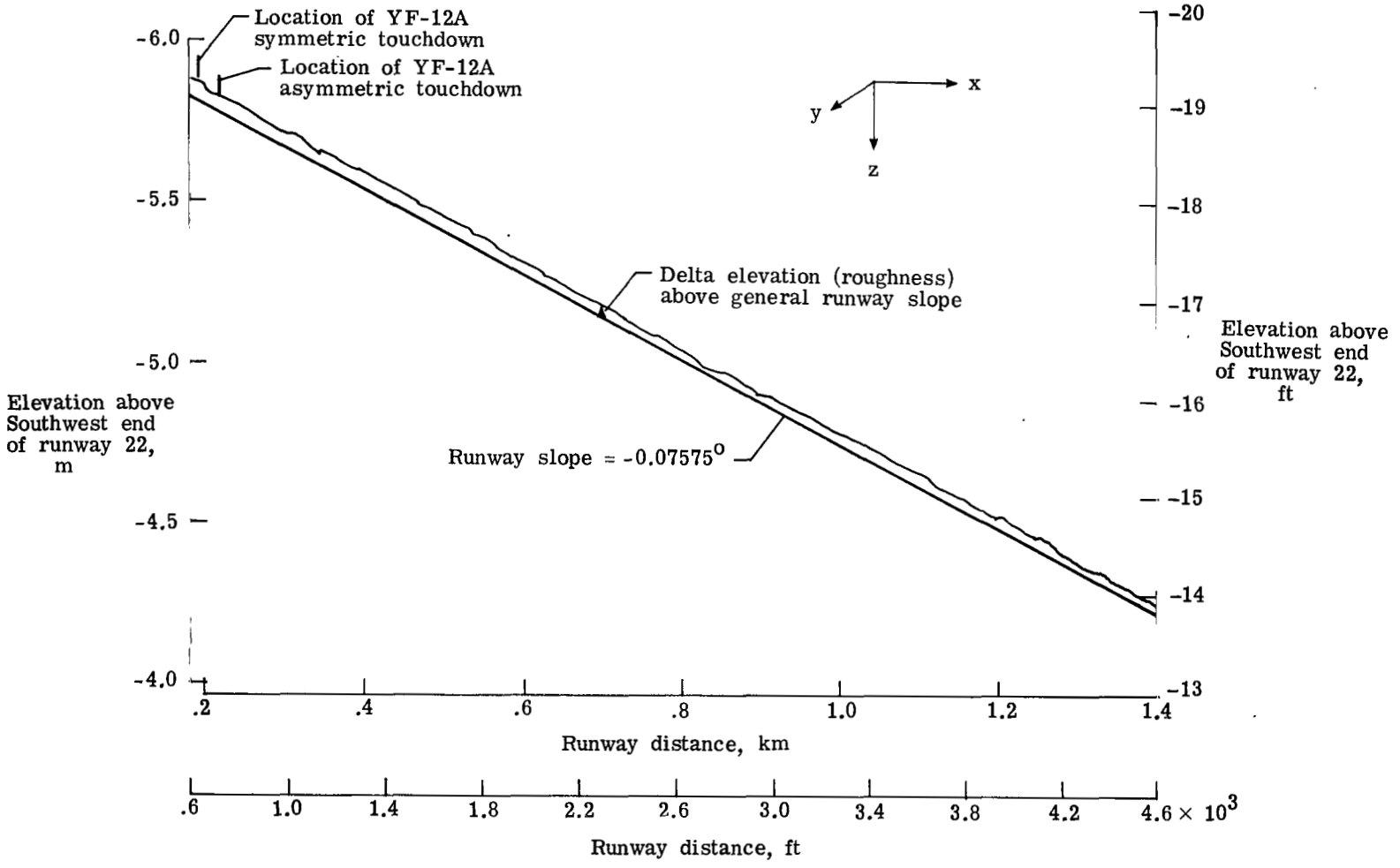

Figure 4.- Characteristics of a 1219-m (4000-ft) section of runway 22 at Edwards Air Force Base, California.

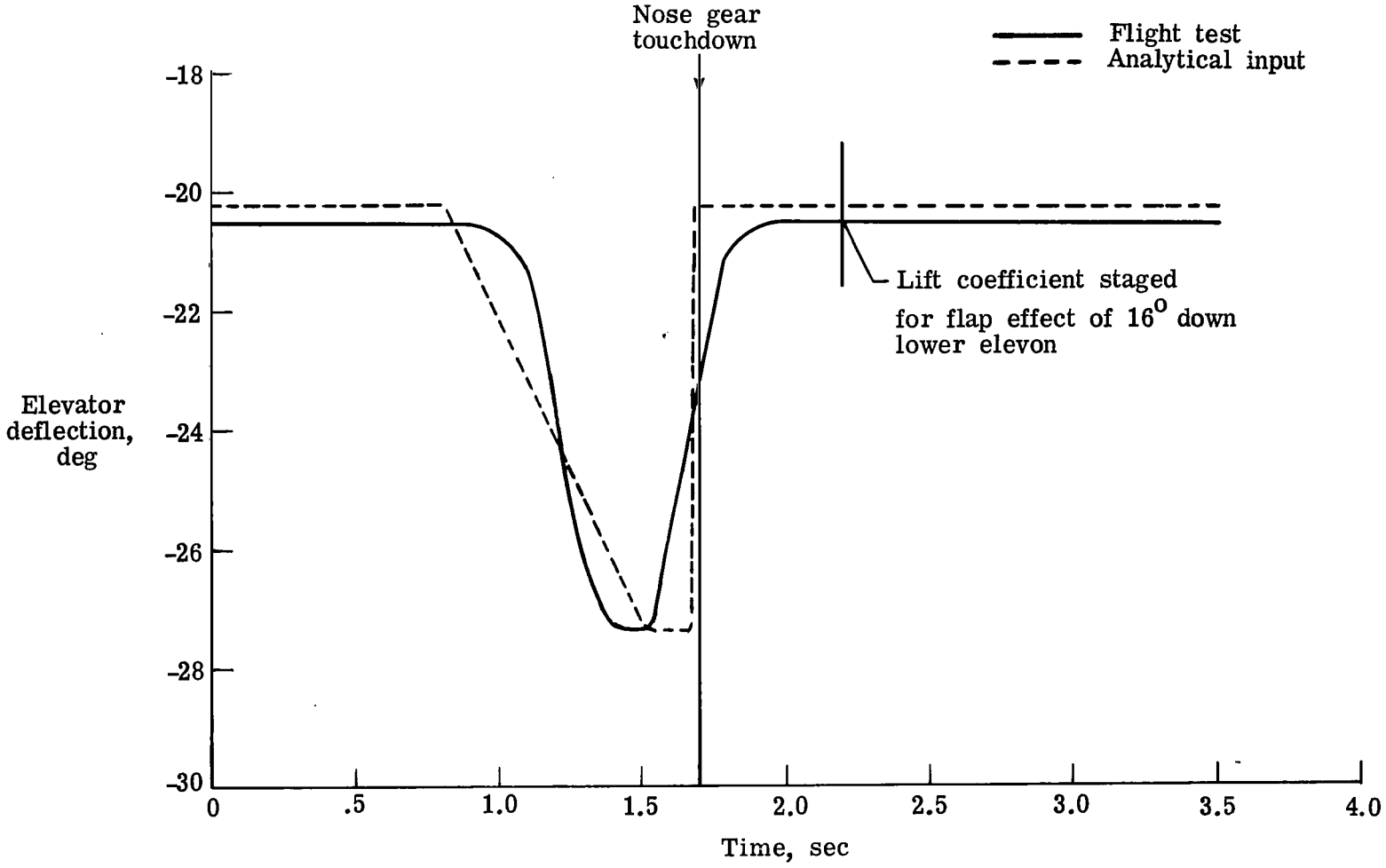

(a) Elevator deflection.

Figure 5.- Analytical rigid body and flight test data for X-24B vehicle.

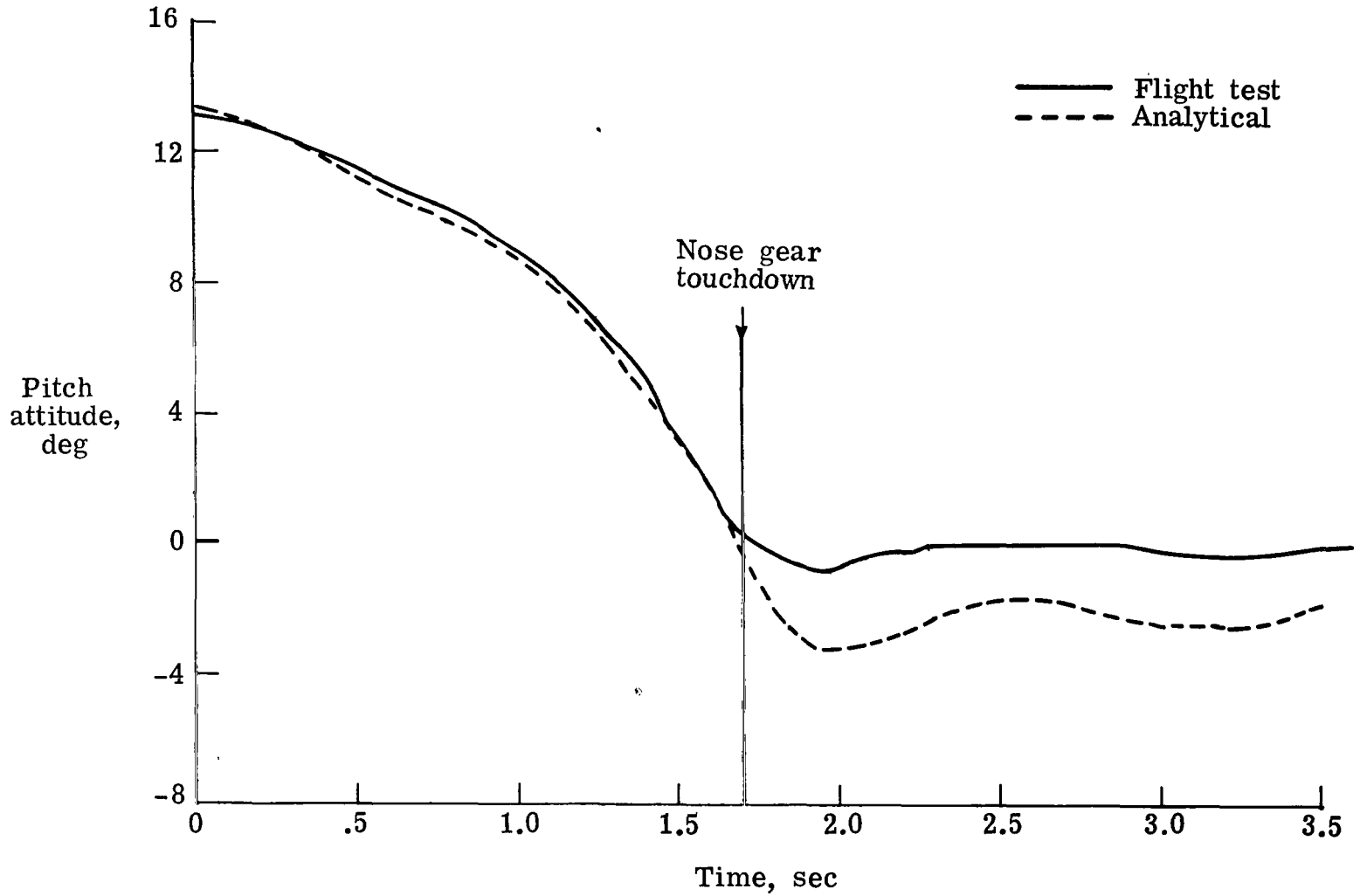

(b) Pitch attitude.

Figure 5.- Continued.

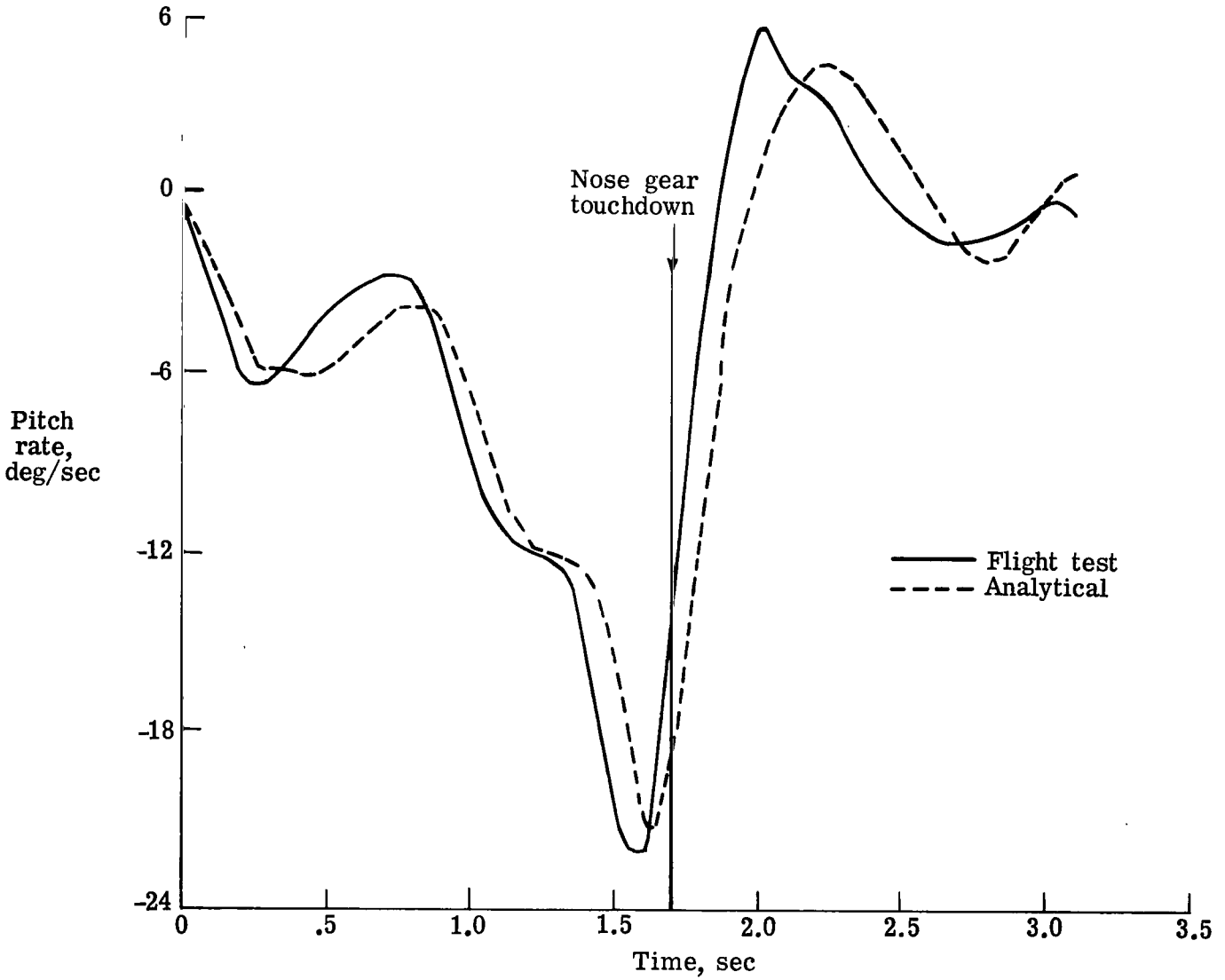

(c) Pitch rate.

Figure 5.- Continued.

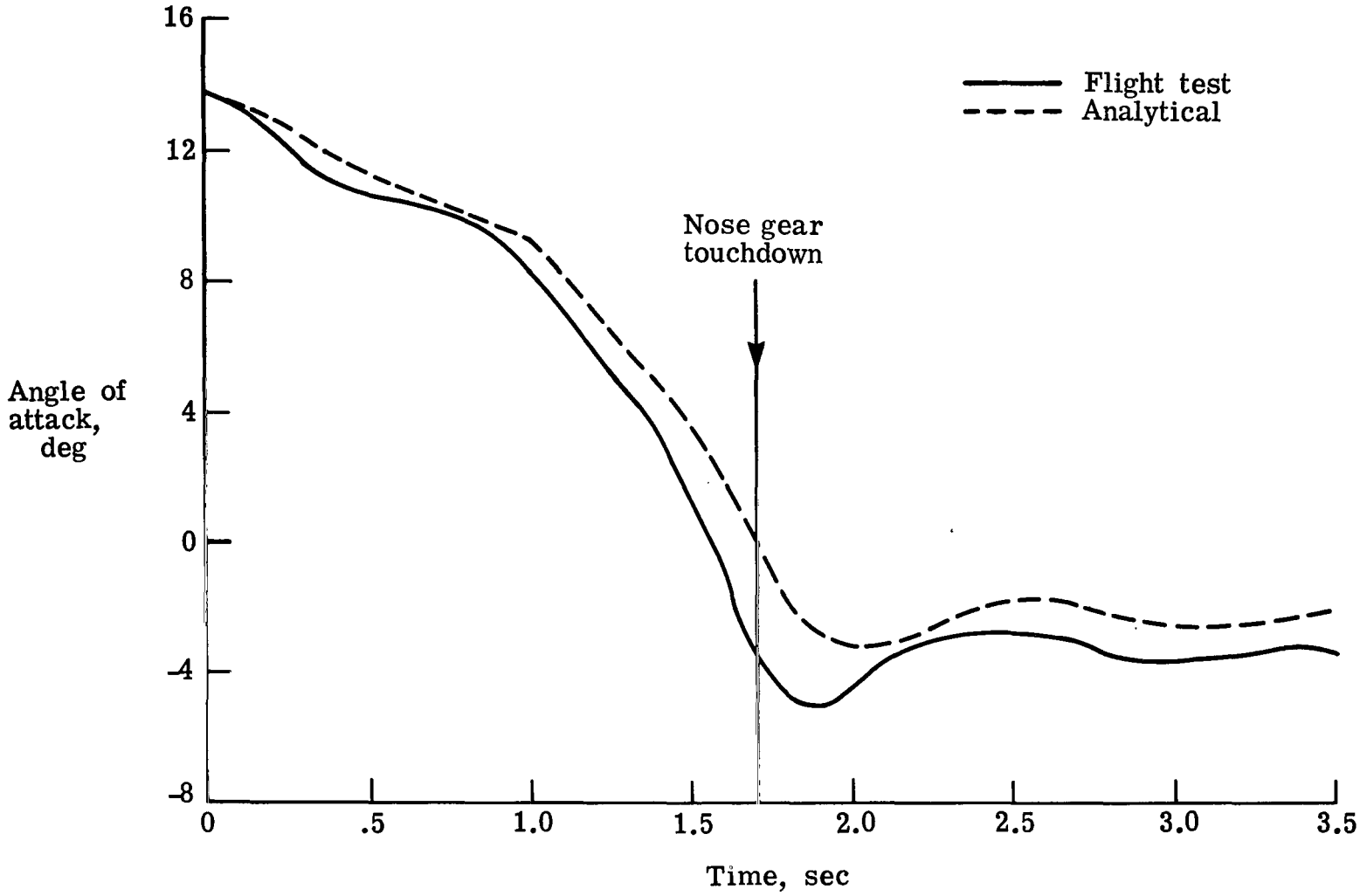

(d) Angle of attack.

Figure 5.- Continued.

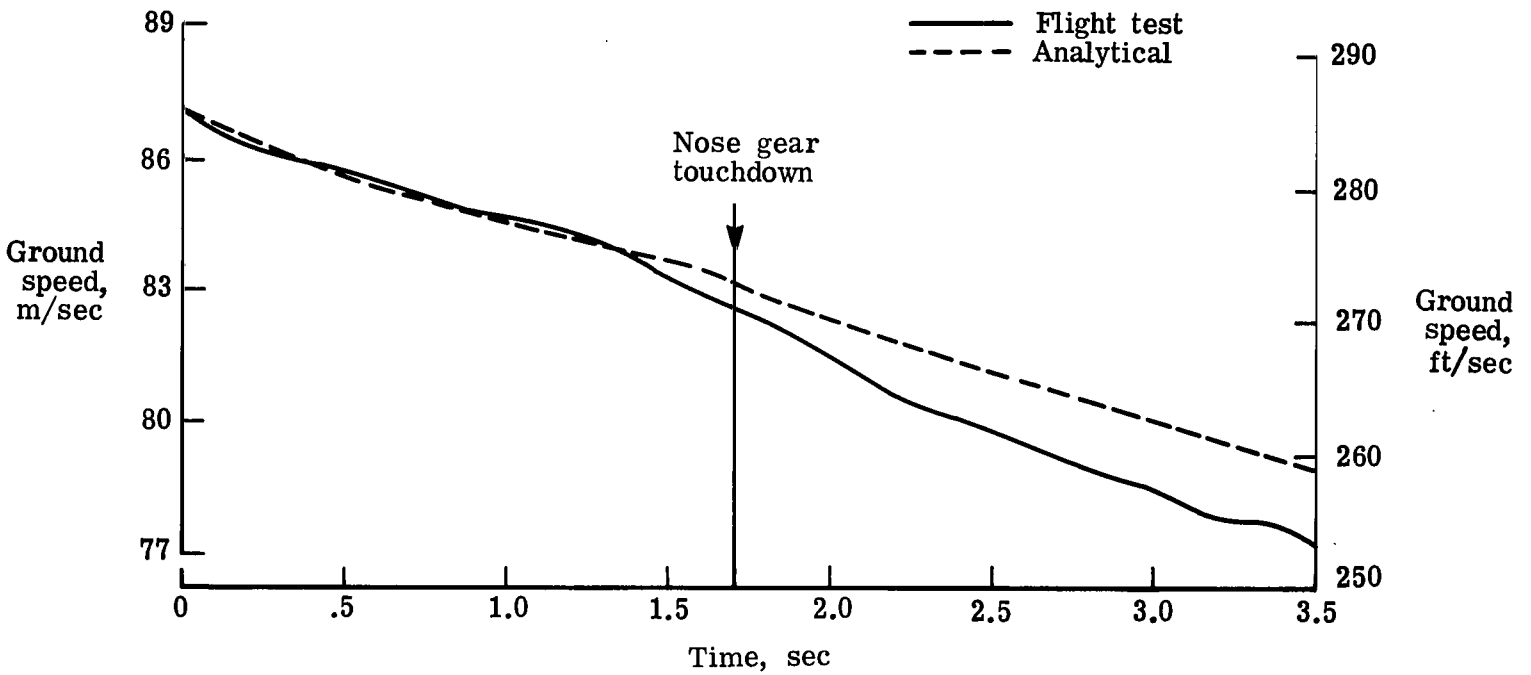

(e) Ground speed.

Figure 5.- Continued.

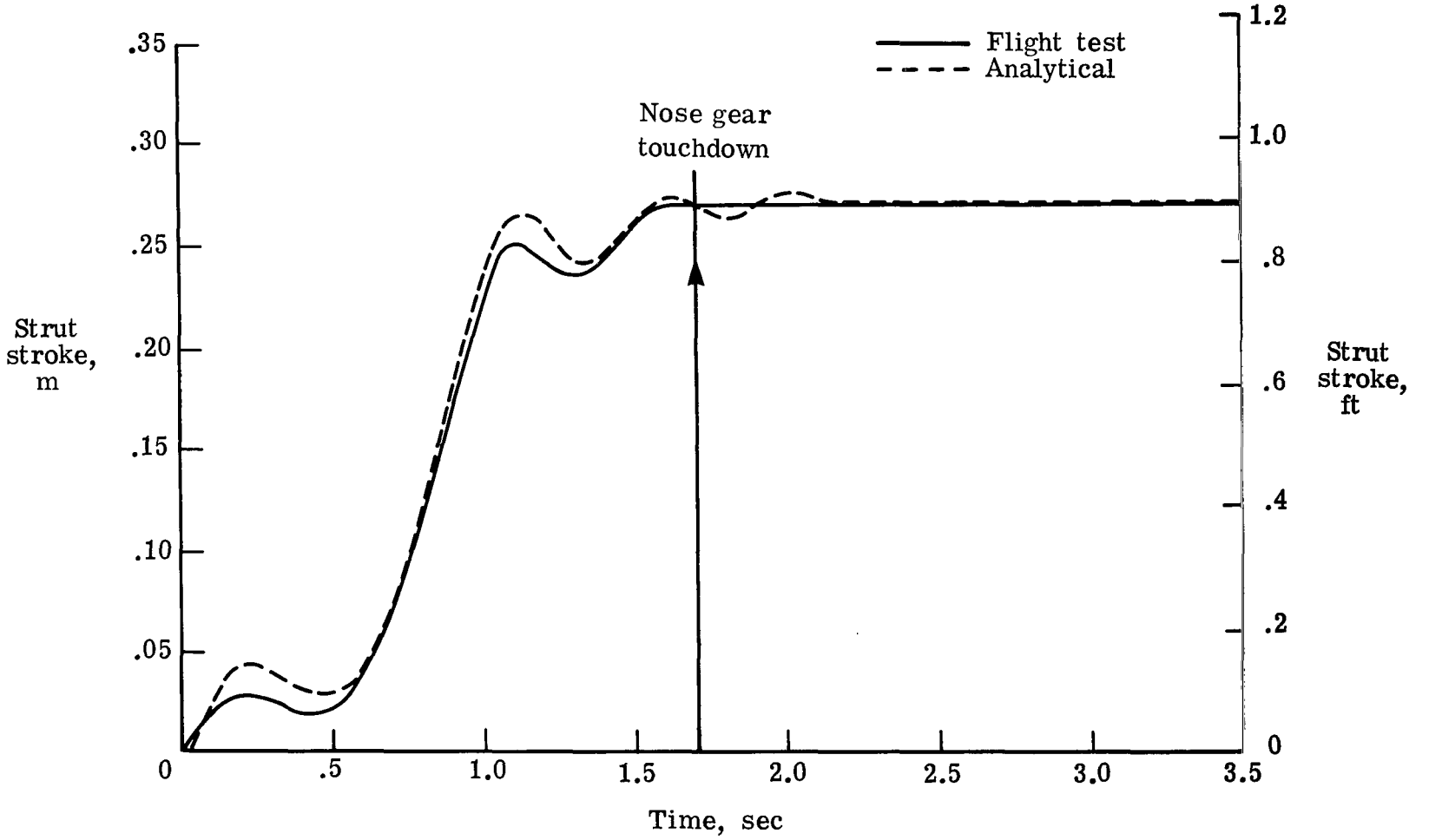

(f) Right main gear strut stroke.

Figure 5.- Continued.

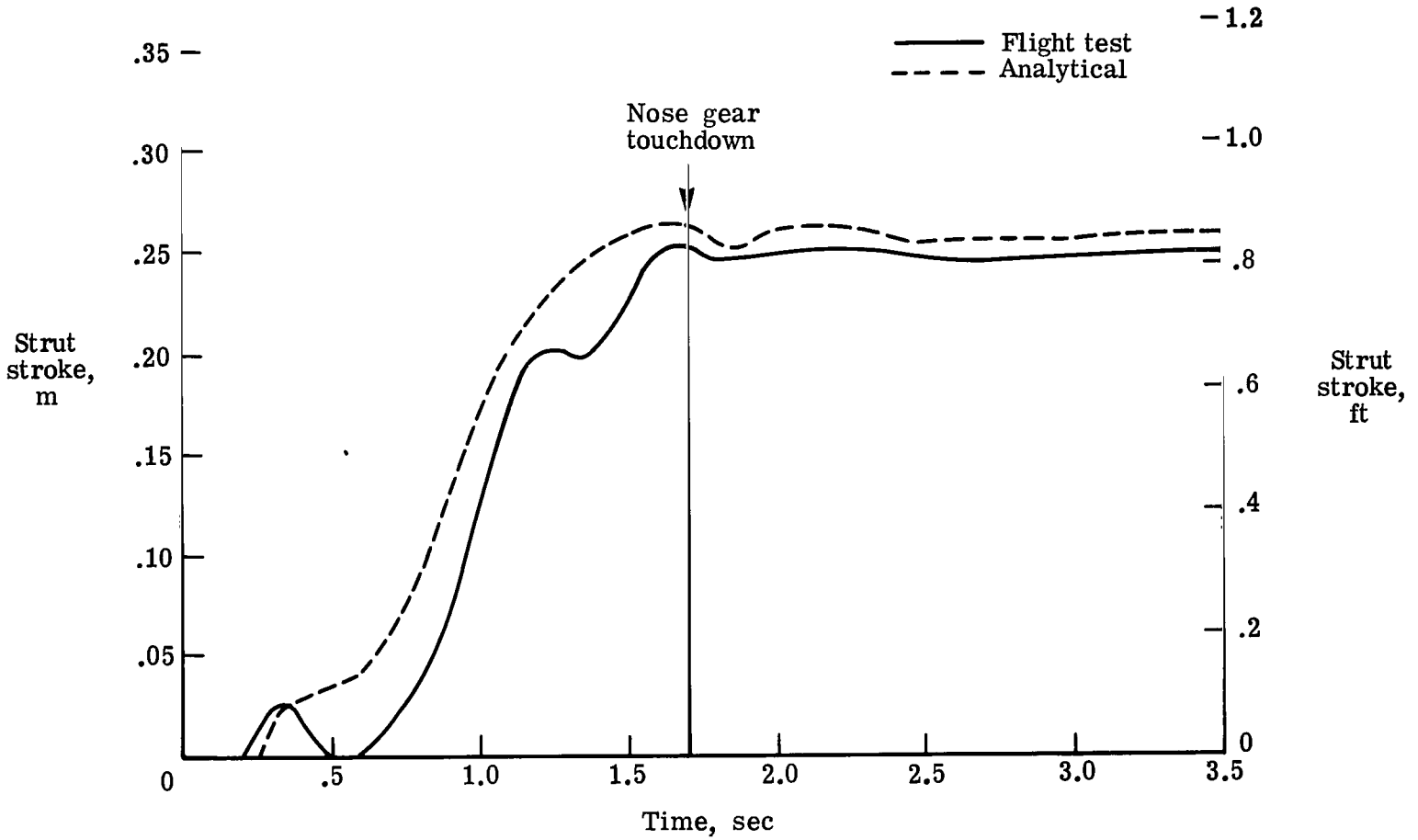

(g) Left main gear strut stroke.

Figure 5.- Continued.

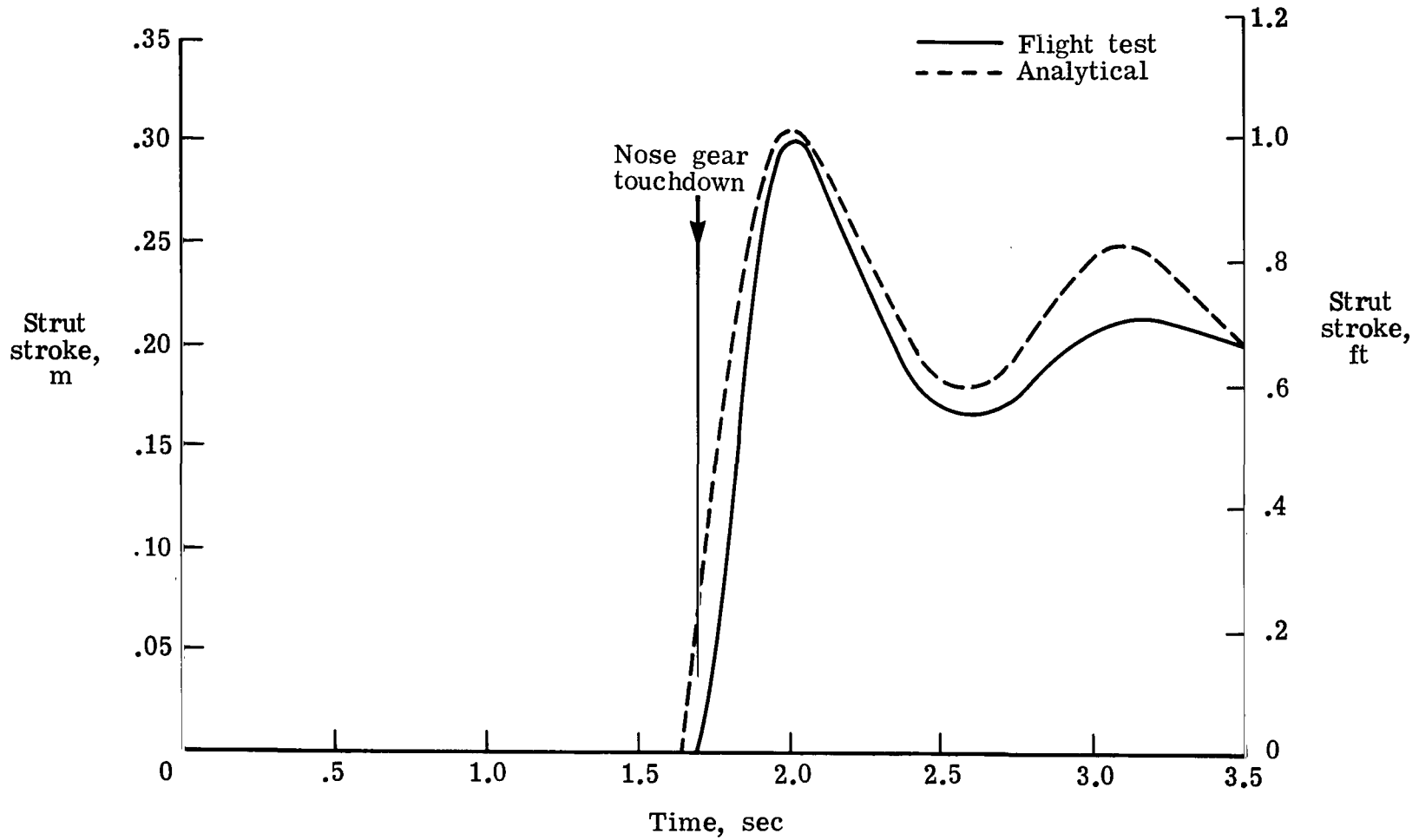

(h) Nose gear strut stroke.

Figure 5.- Continued.

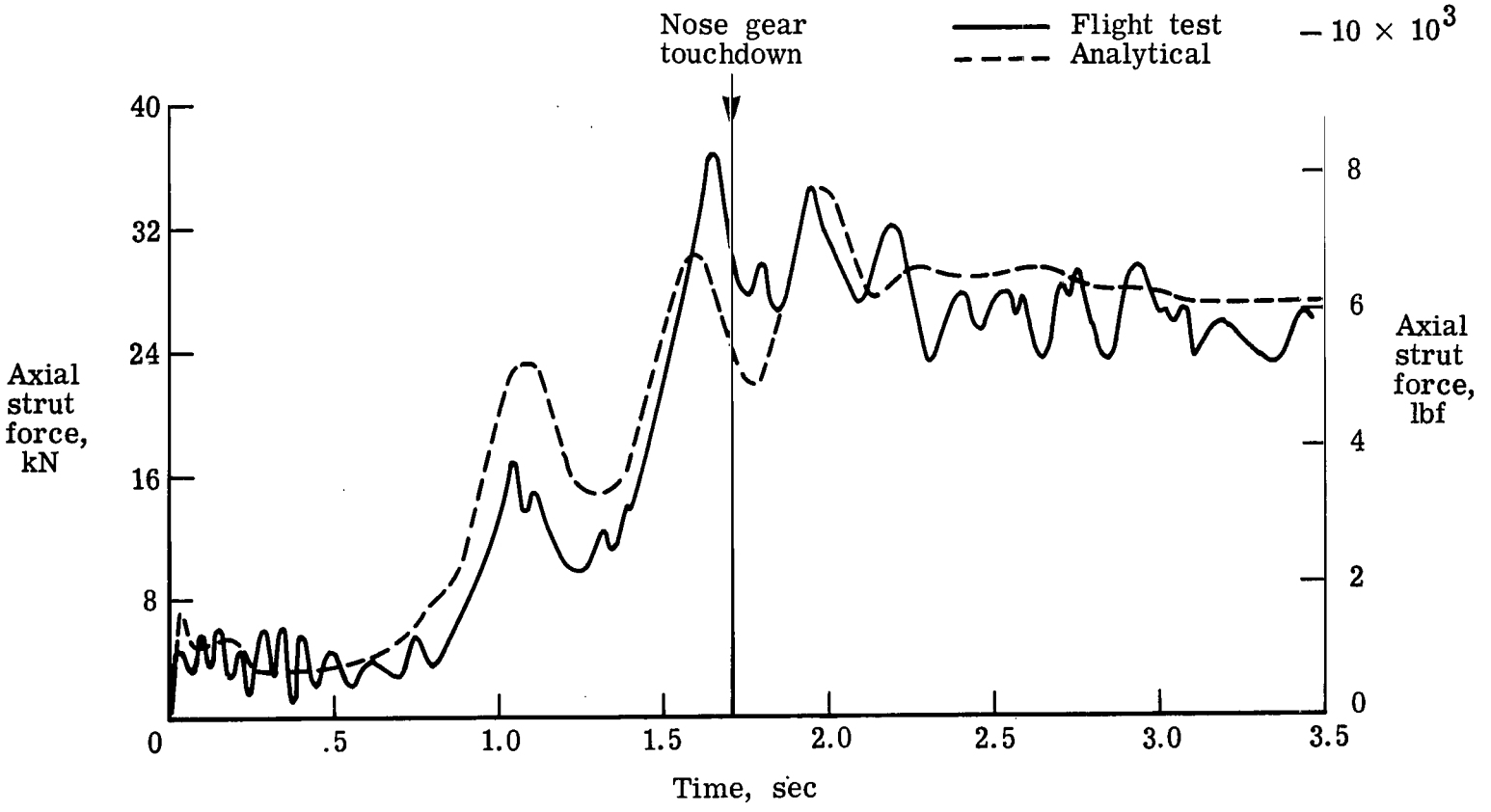

(i) Right main gear axial strut force.

Figure 5.- Continued.

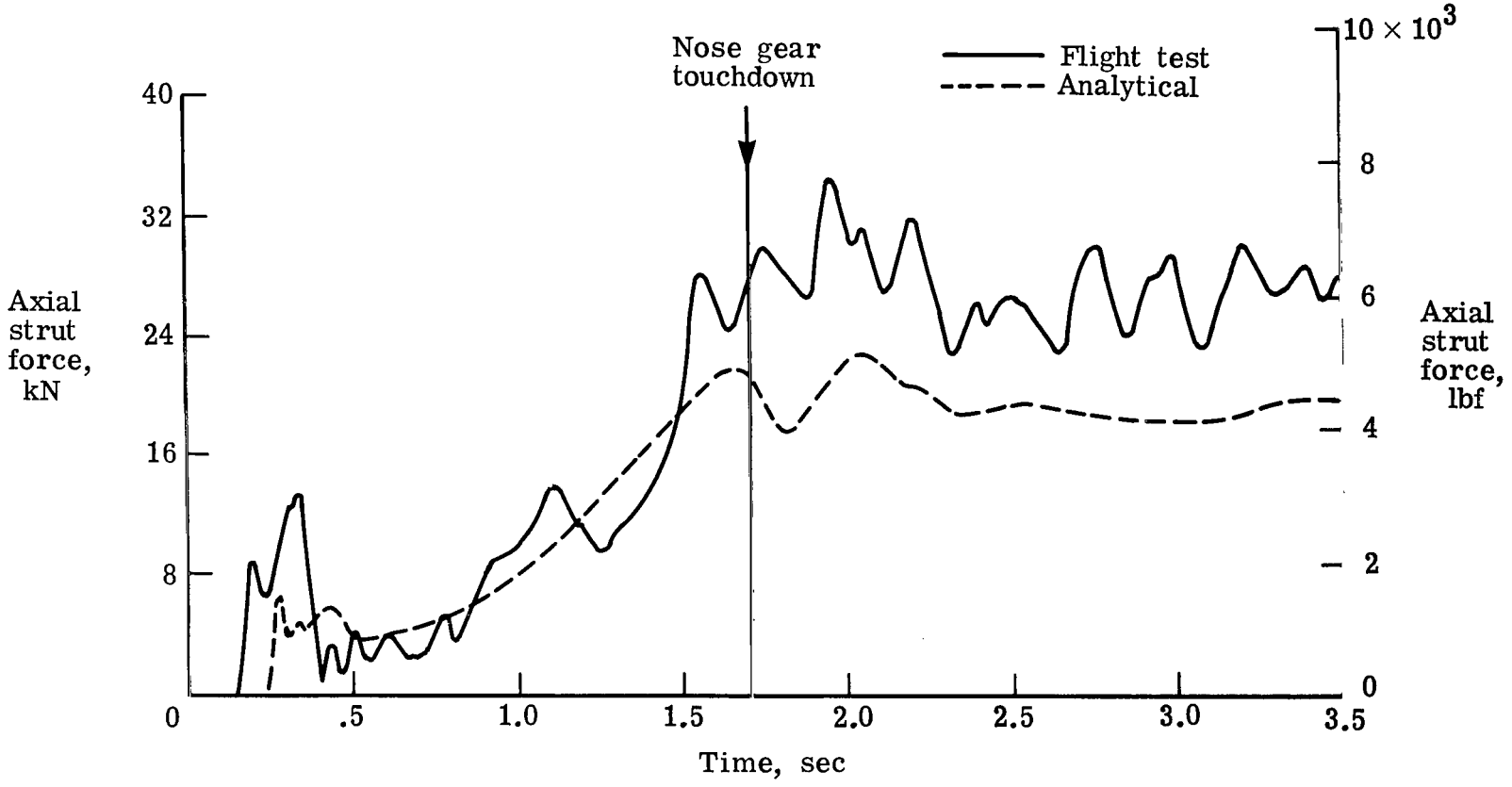

(j) Left main gear axial strut force.

Figure 5.- Continued.

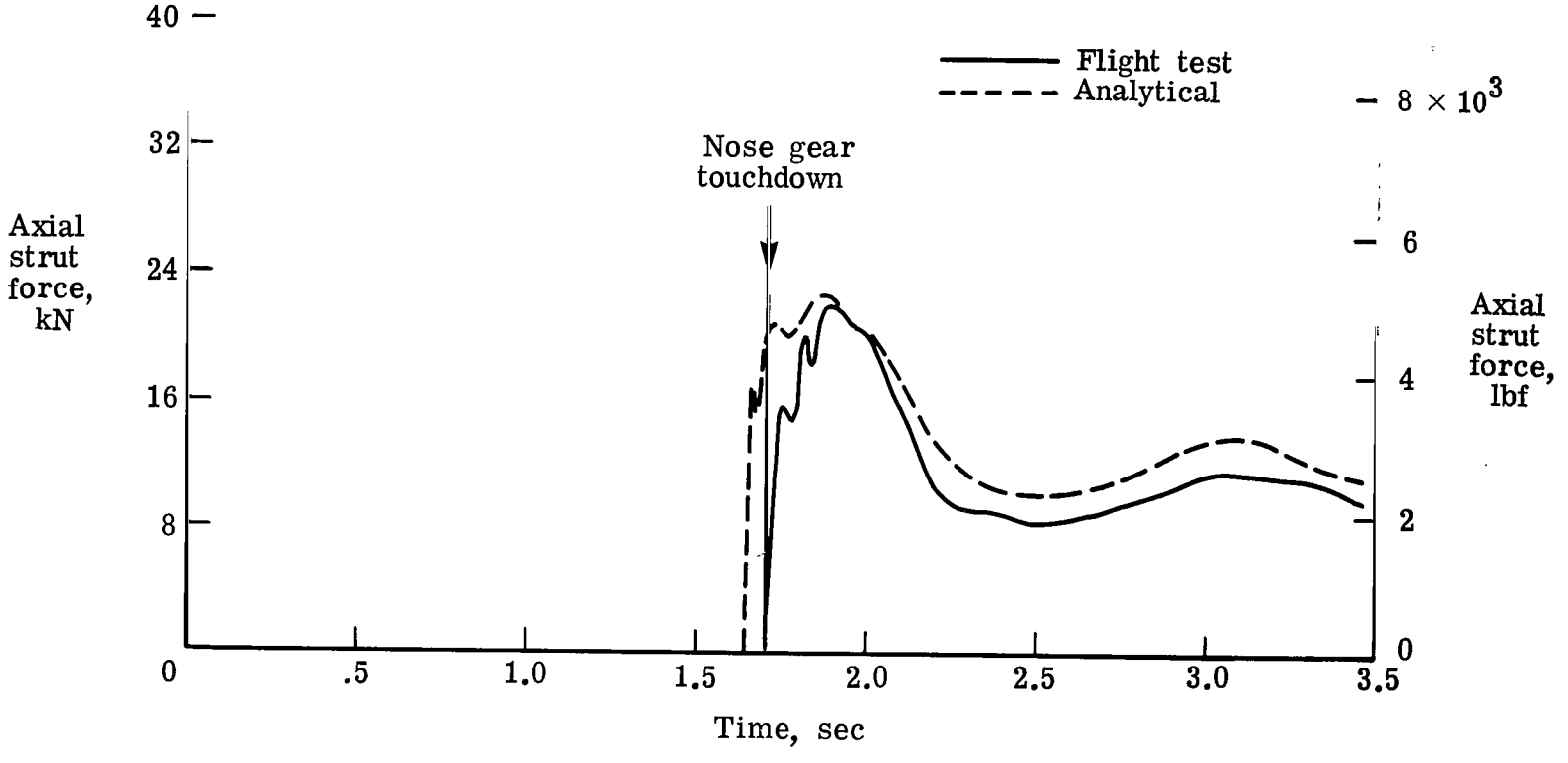

(k) Nose gear axial strut force.

Figure 5.- Concluded.

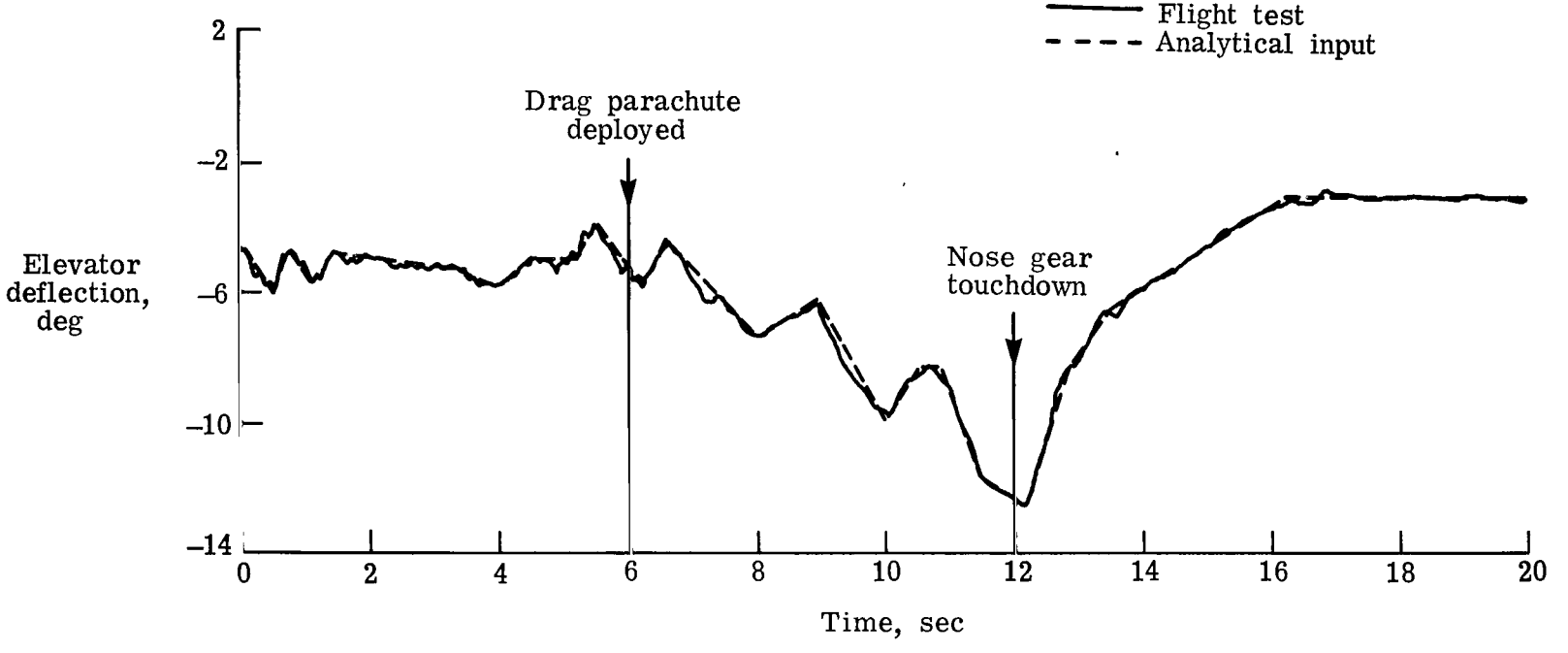

(a) Elevator deflection.

Figure 6.- Analytical flexible body and flight-test data for symmetric touchdown of YF-12A airplane.

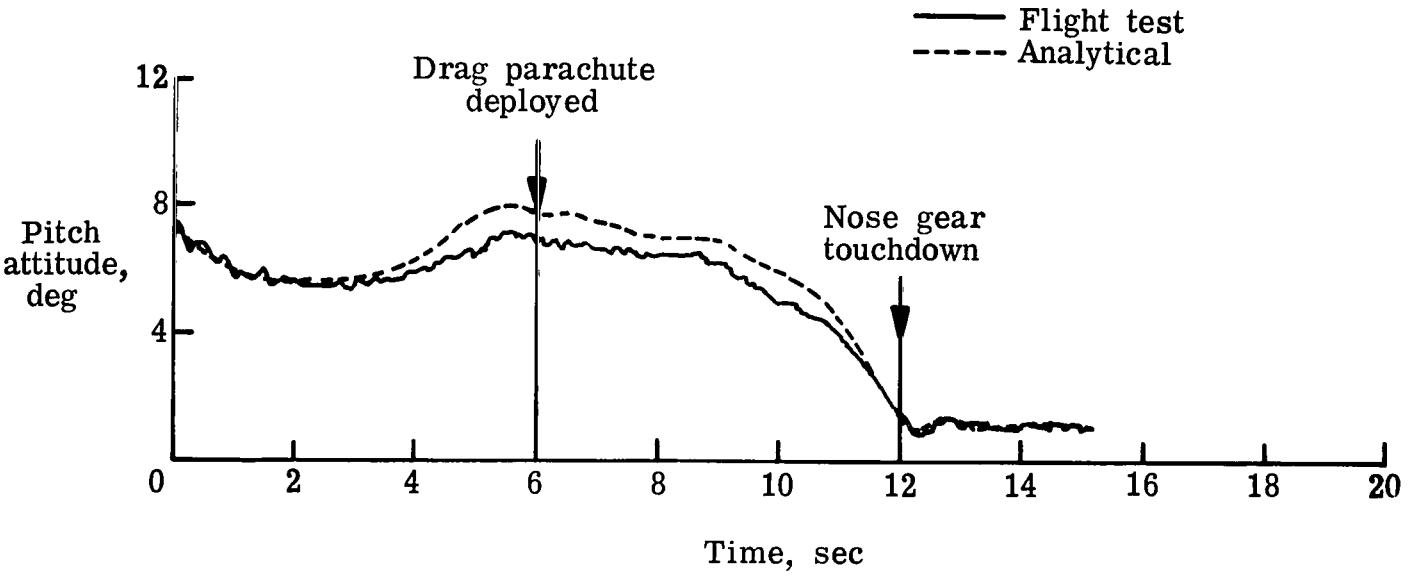

(b) Pitch attitude.

Figure 6.- Continued.

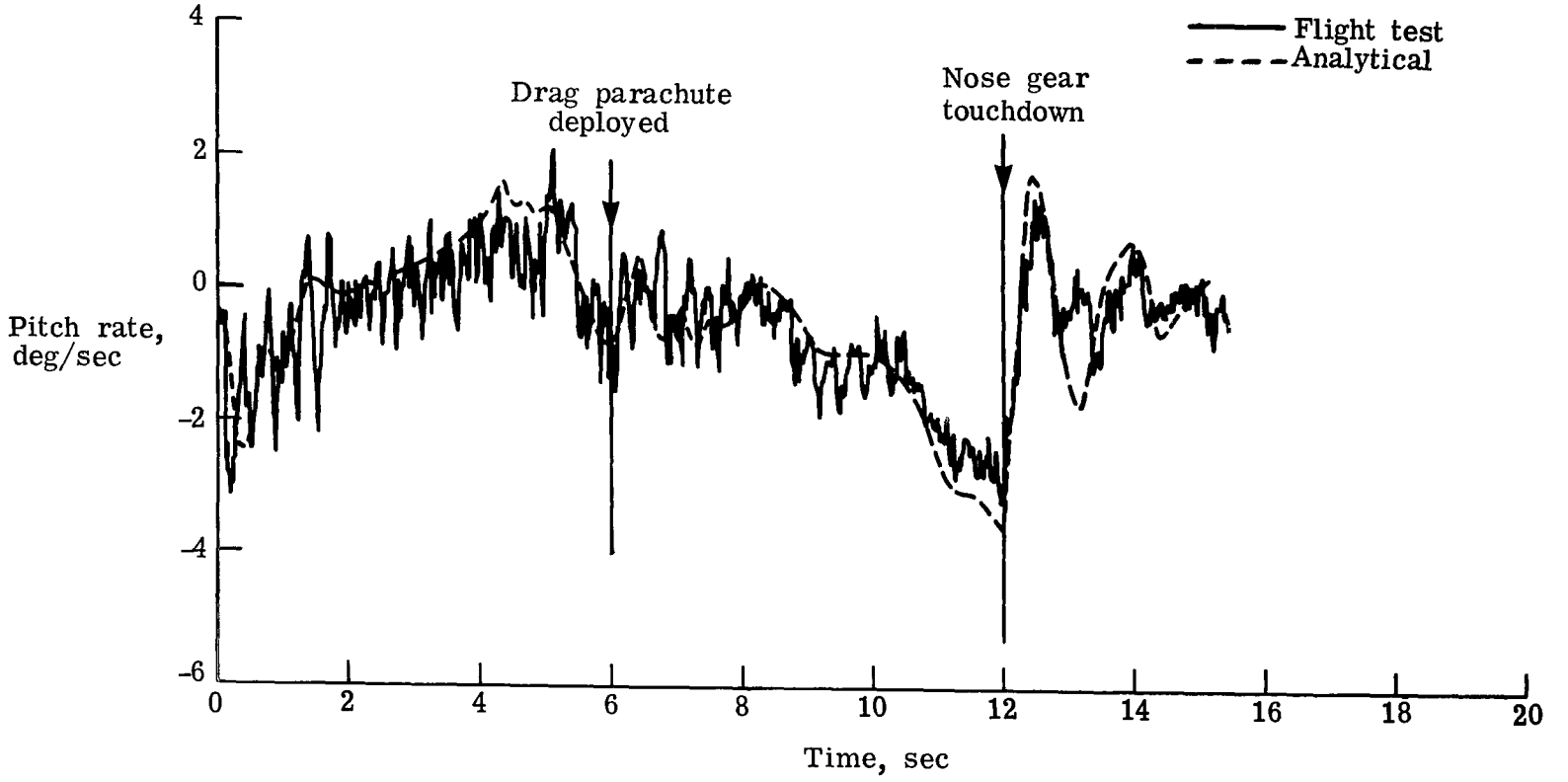

(c) Pitch rate.

Figure 6.- Continued.

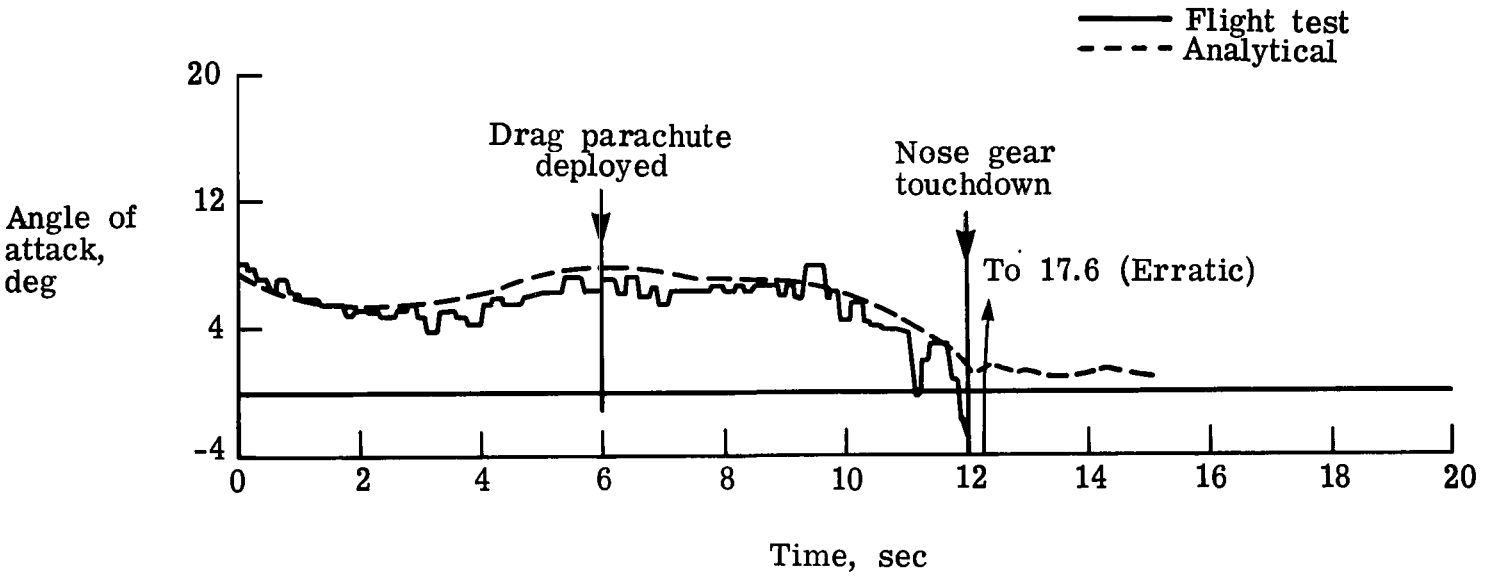

(d) Angle of attack.

Figure 6.- Continued.

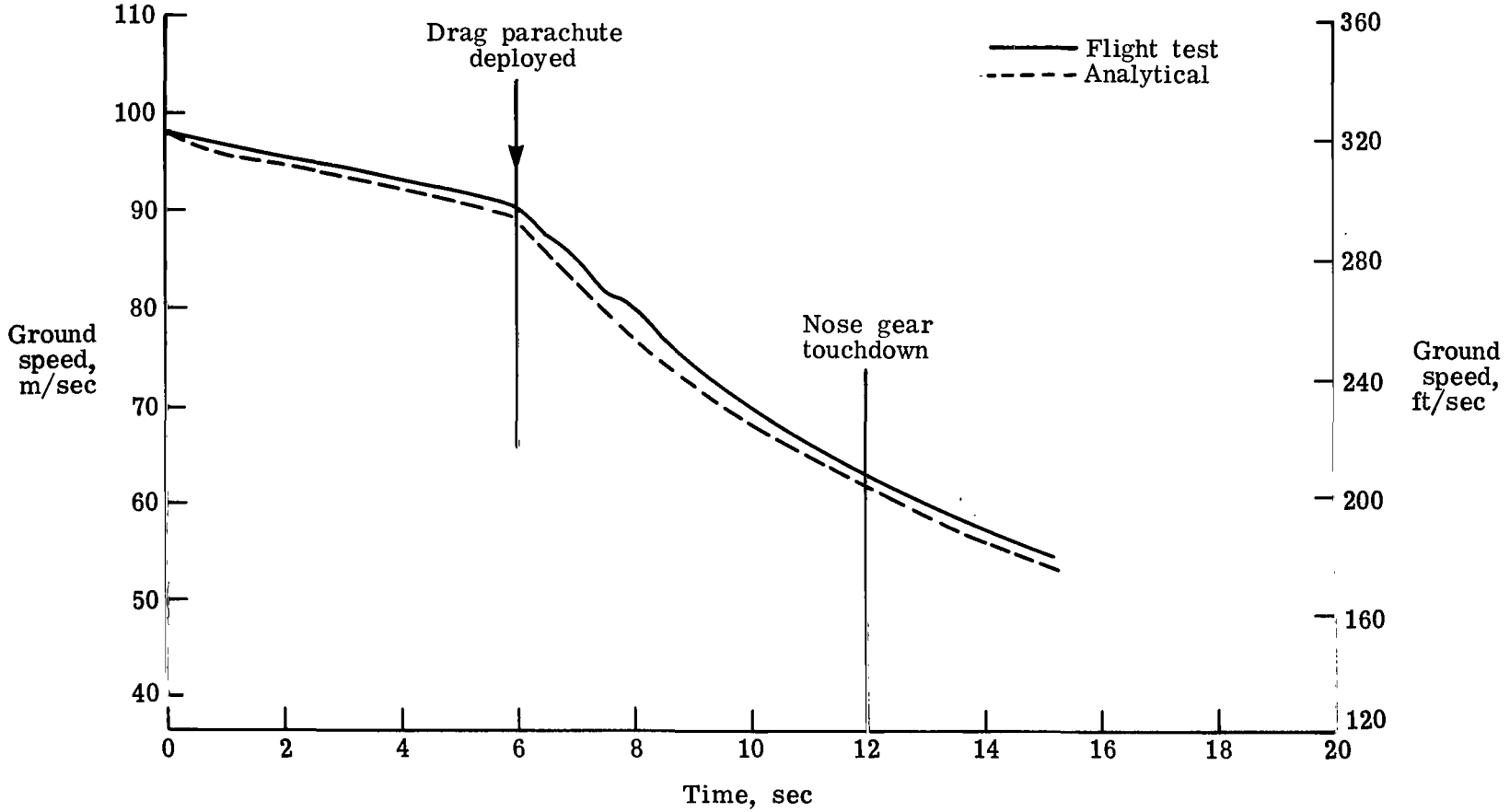

(e) Ground speed.

Figure 6.- Continued.

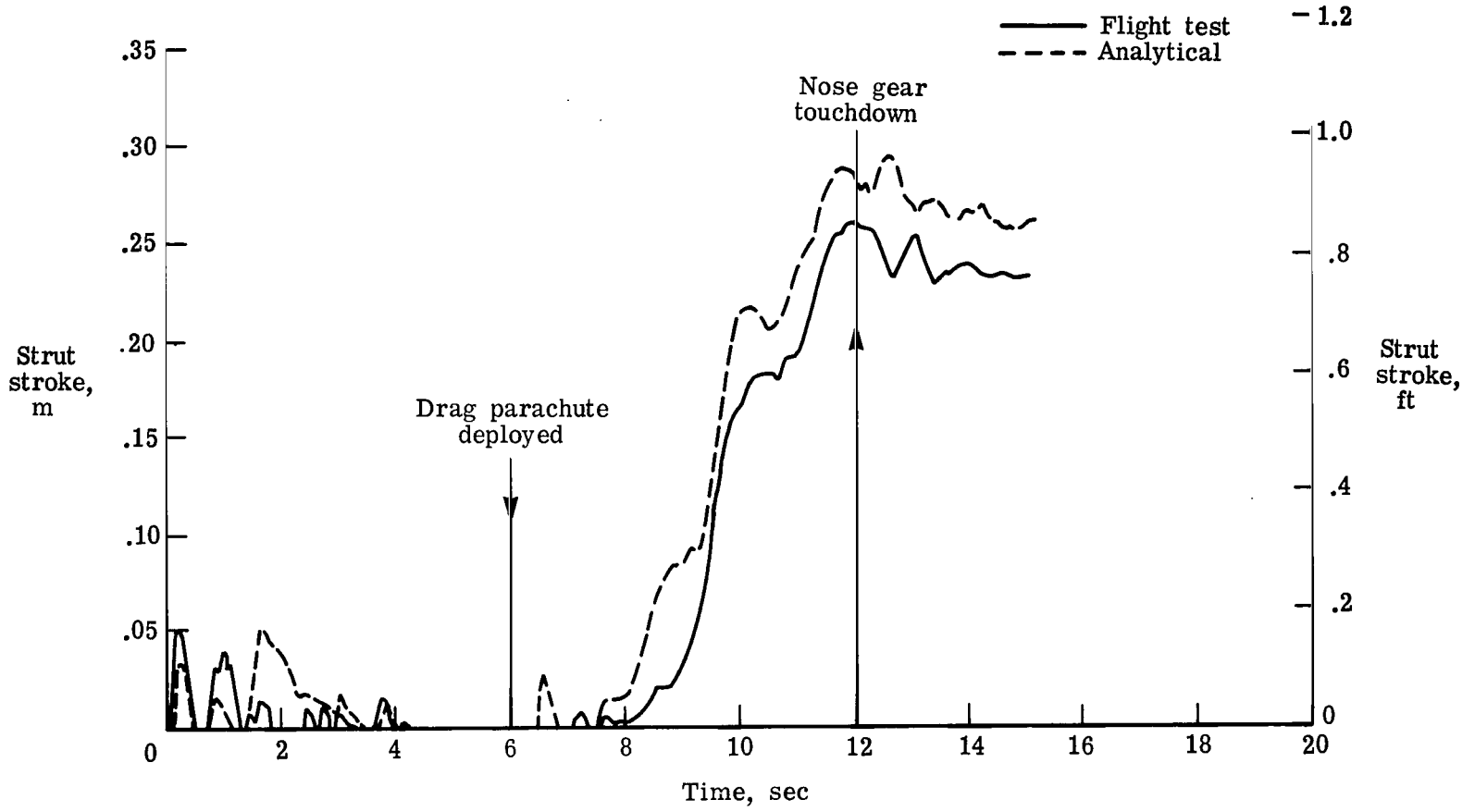

(f) Right main gear strut stroke.

Figure 6.- Continued.

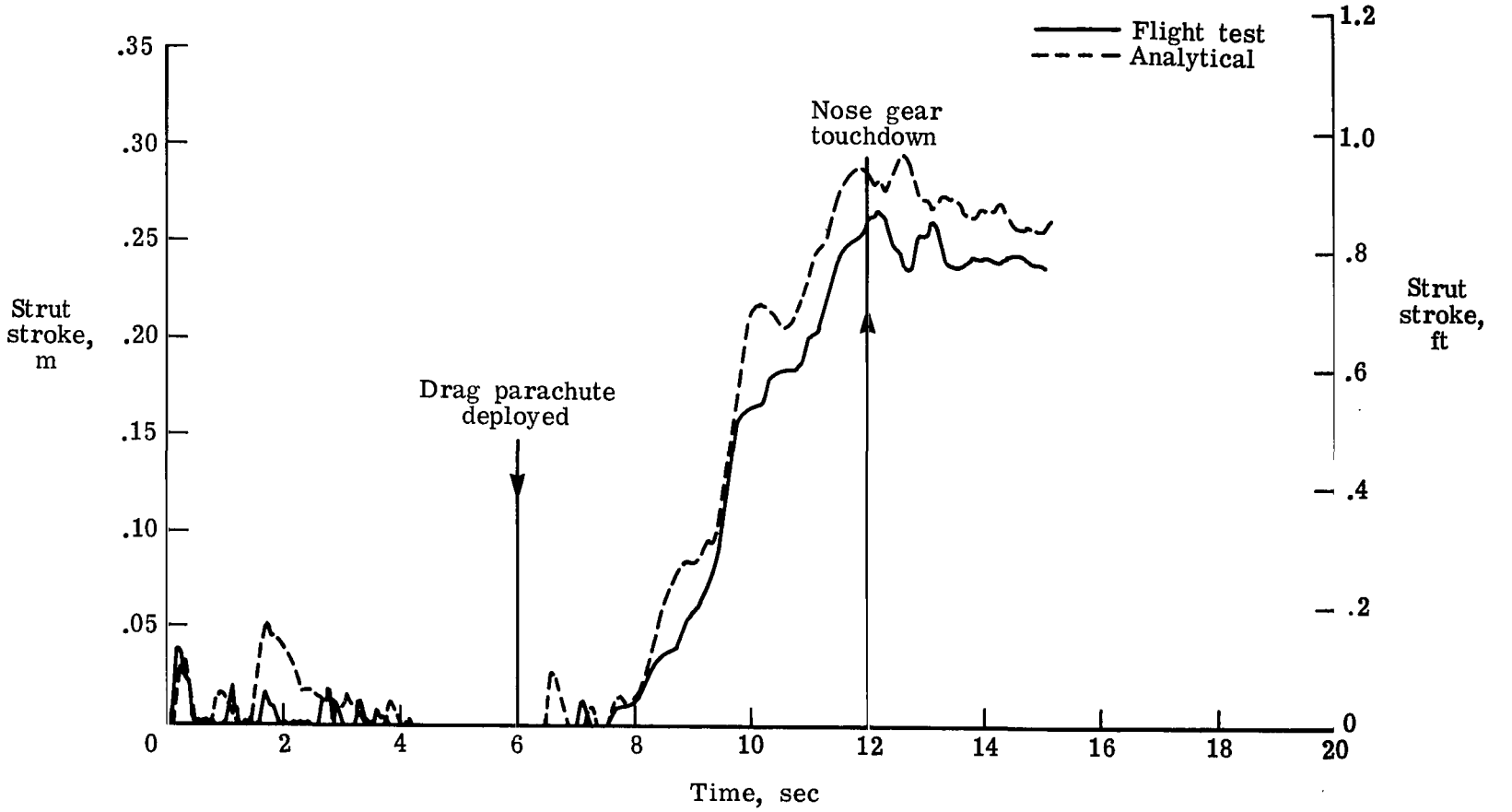

(g) Left main gear strut stroke.

Figure 6.- Continued.

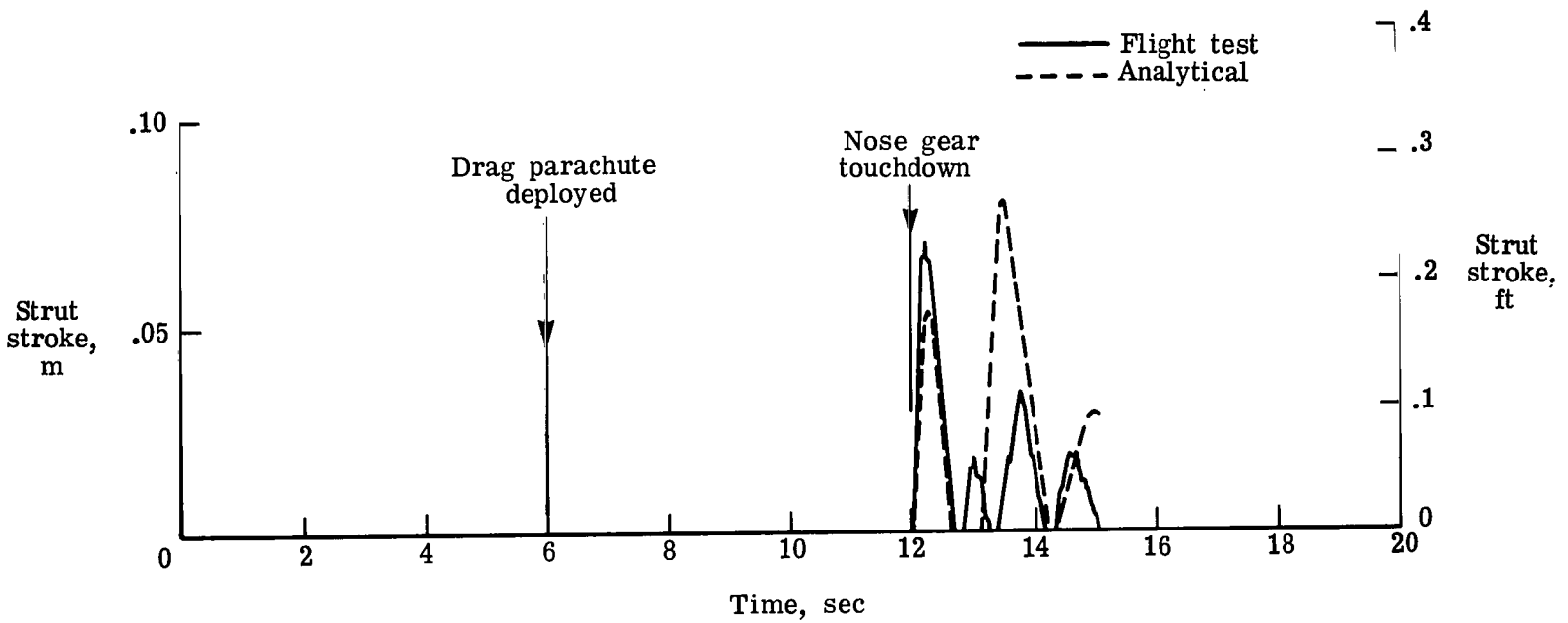

(h) Nose gear strut stroke.

Figure 6.- Continued.

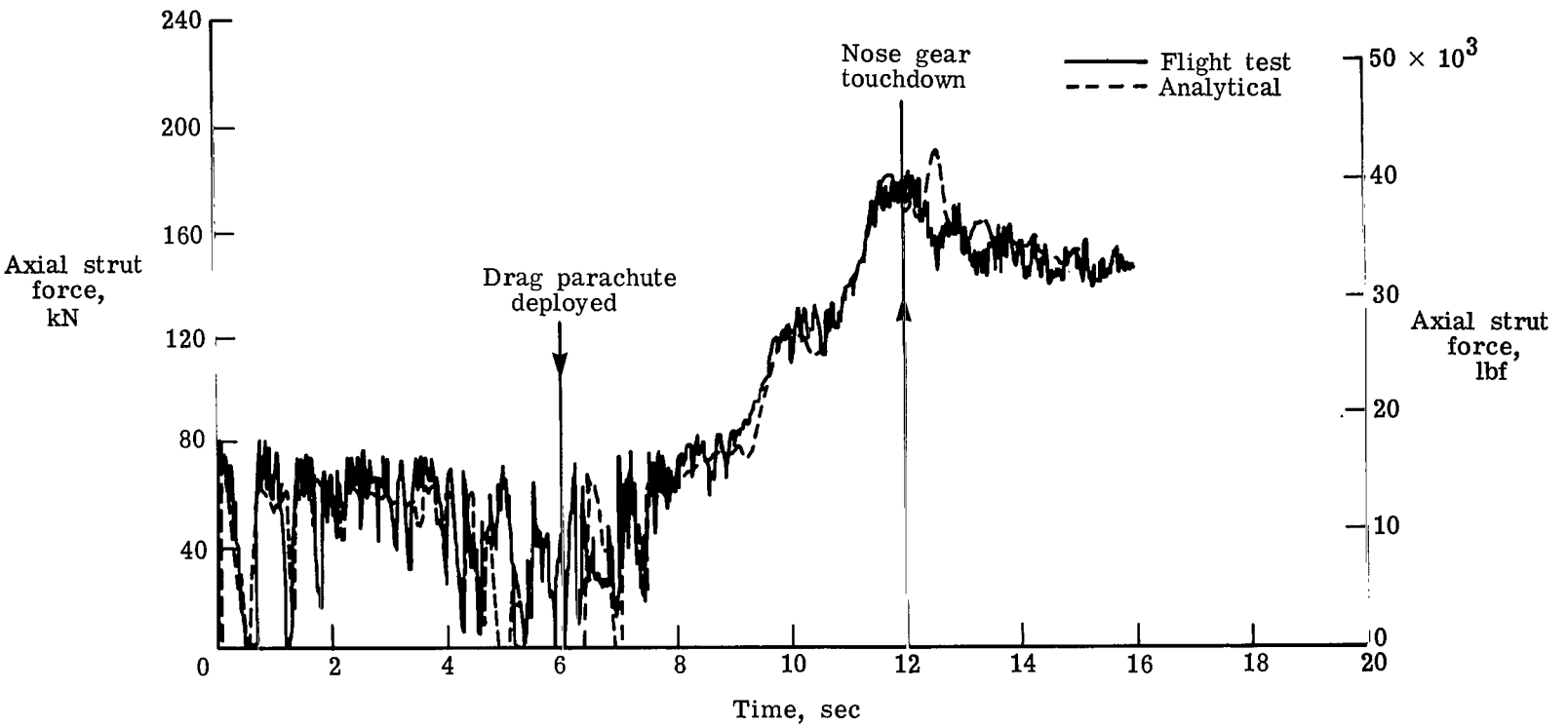

(i) Right main gear axial strut force.

Figure 6.- Continued.

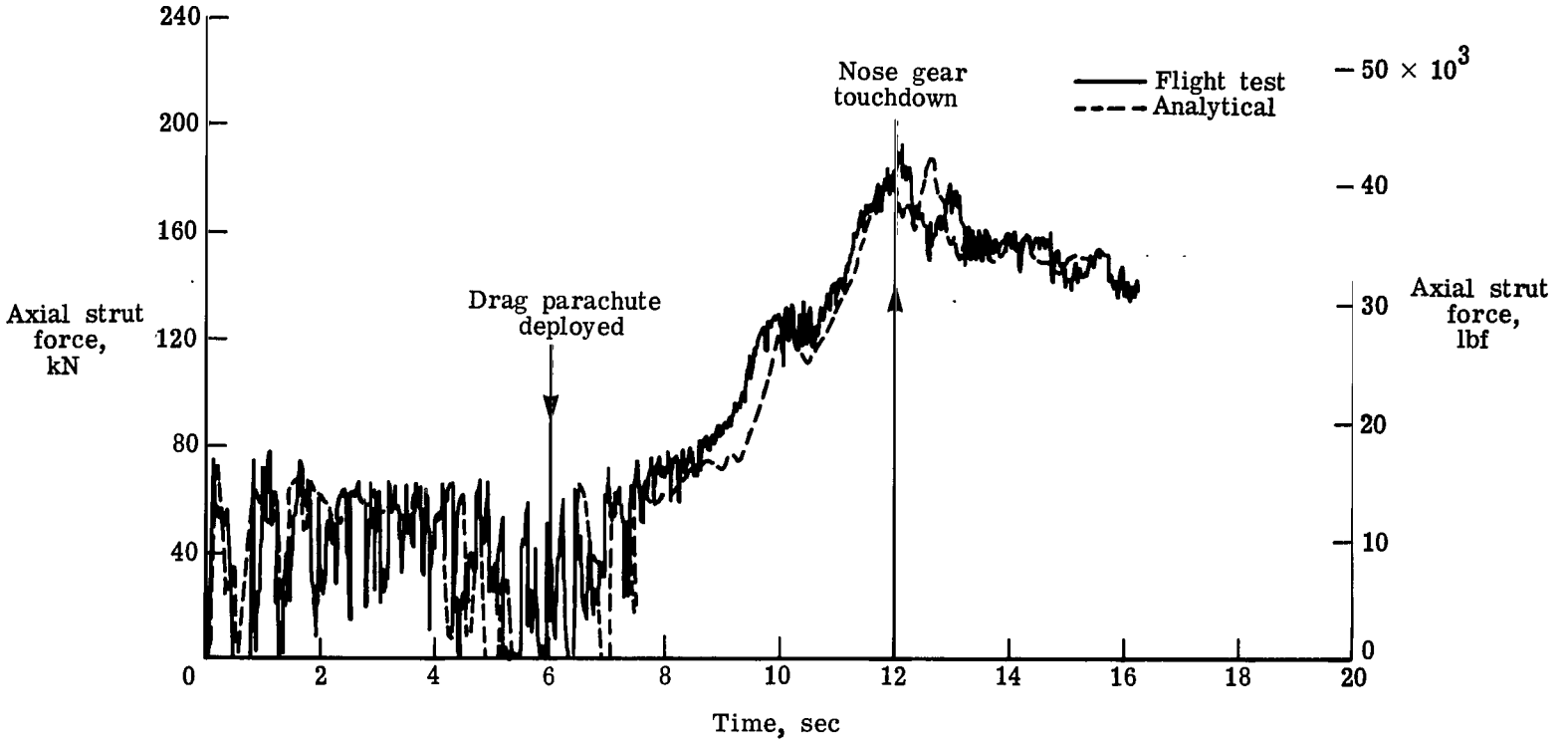

(j) Left main gear axial strut force.

Figure 6.- Continued.

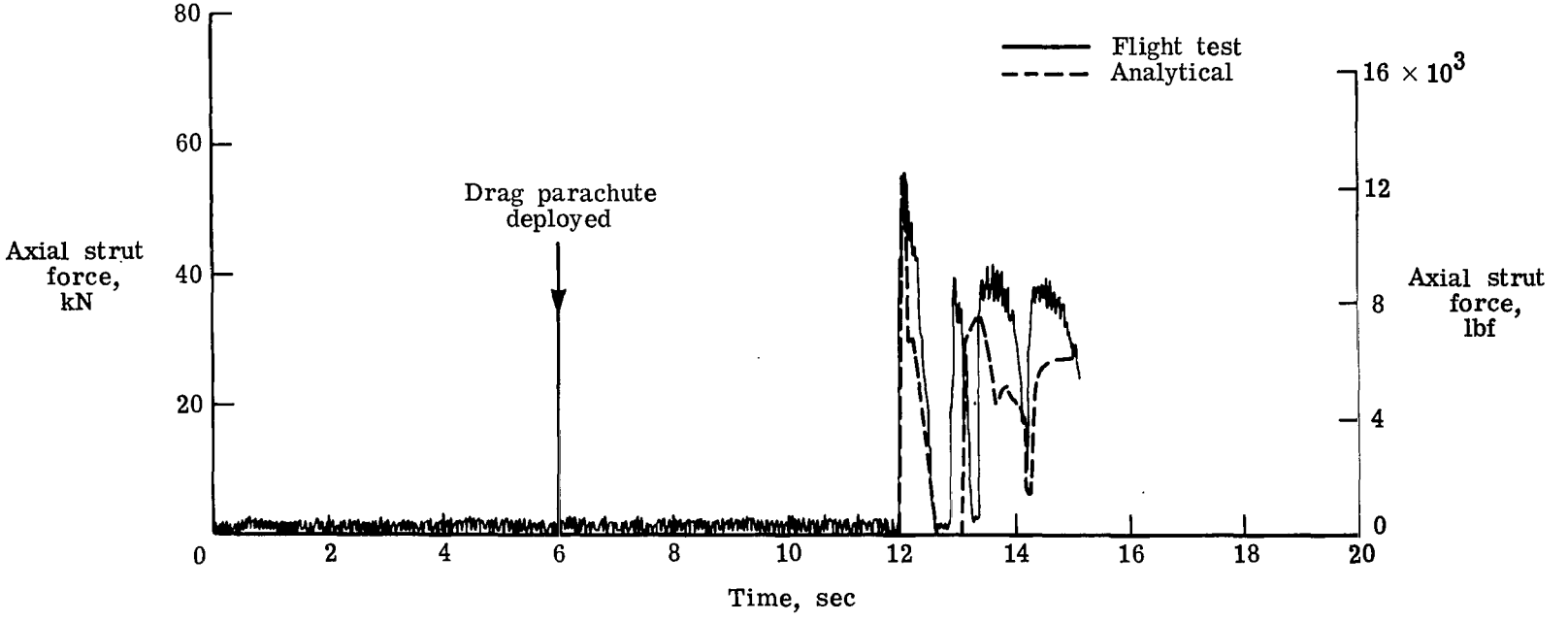

(k) Nose gear axial strut force.

Figure 6.- Continued.

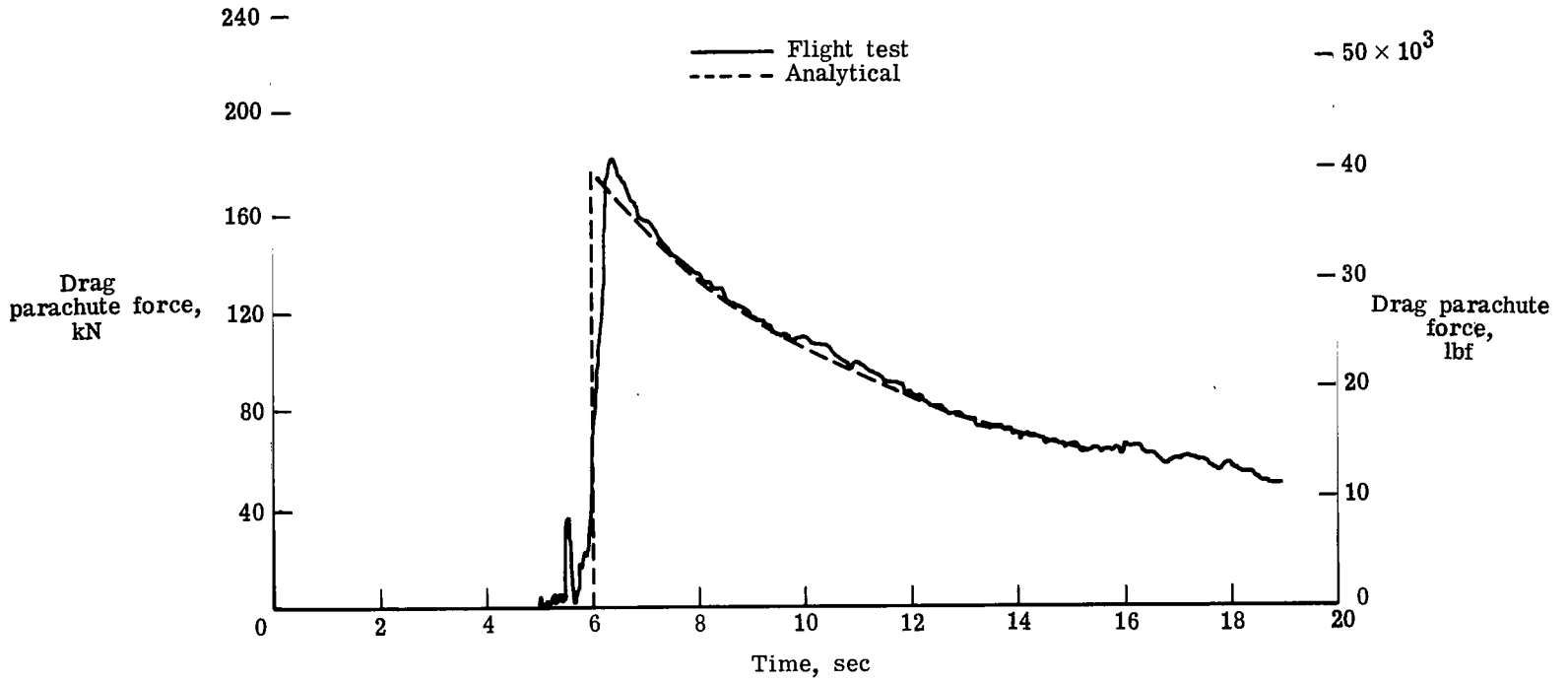

(1) Drag parachute force.

Figure 6.- Continued.

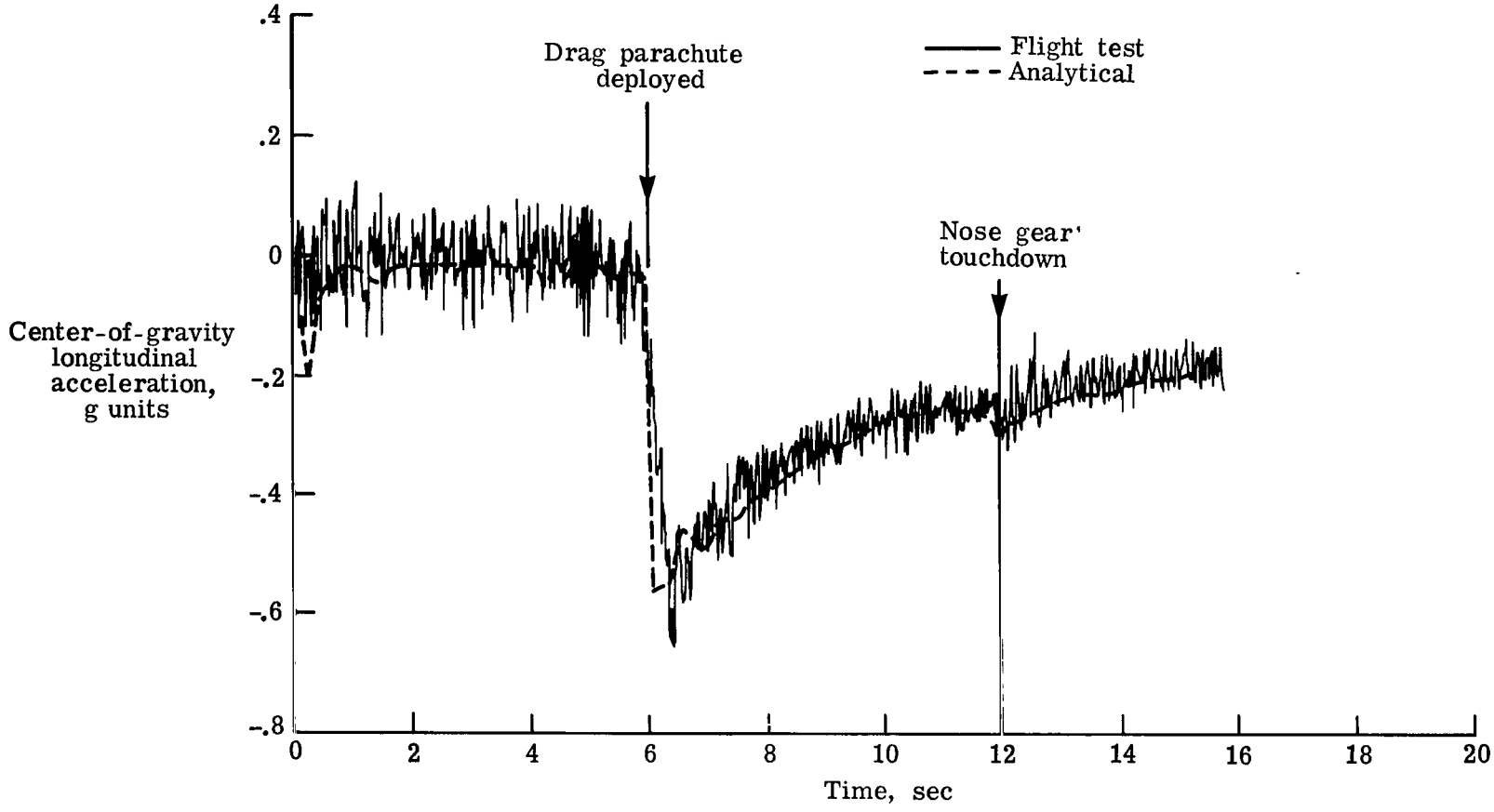

(m) Longitudinal acceleration of center of gravity.

Figure 6.- Continued.

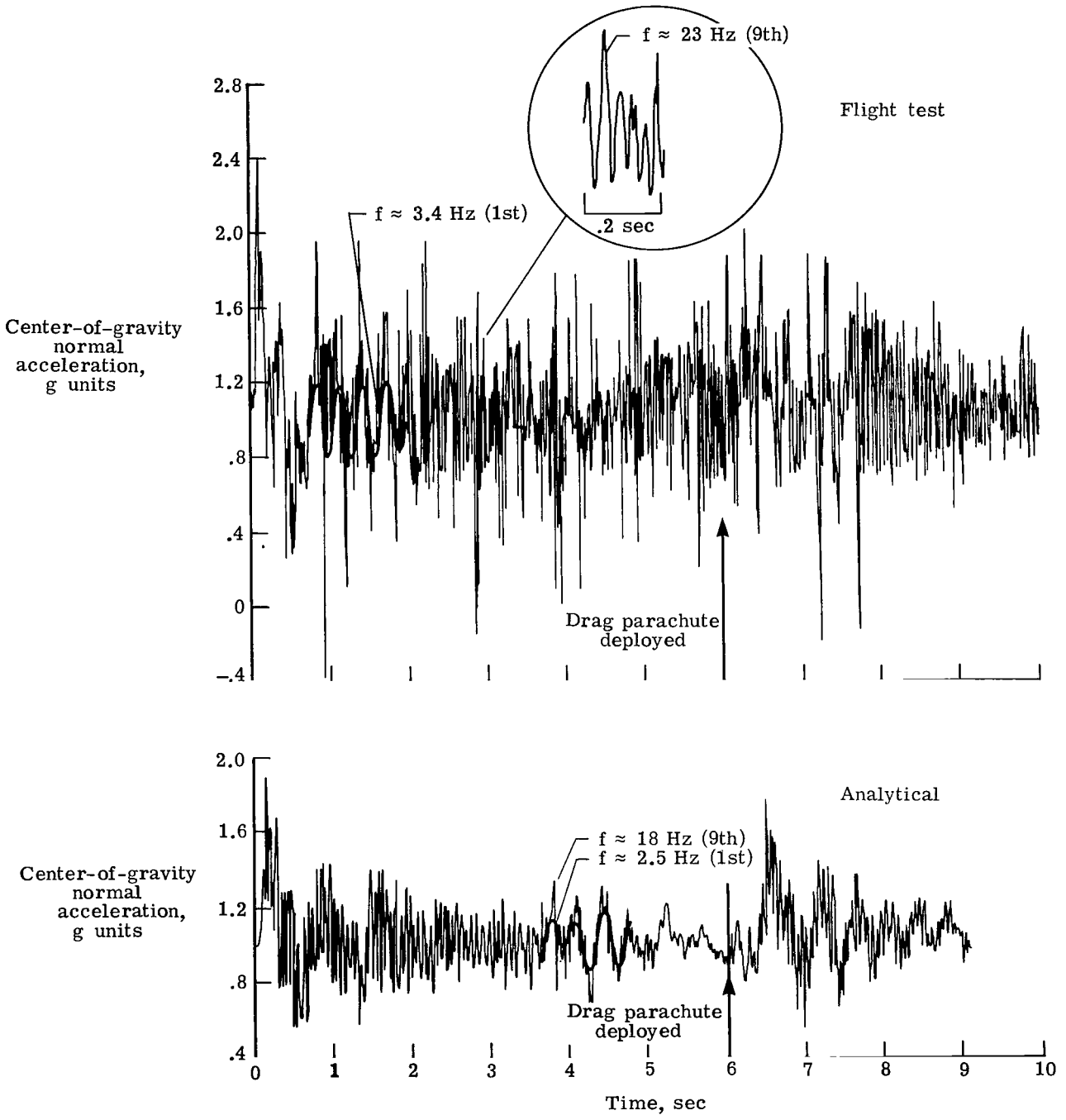

(n) Normal acceleration of center of gravity. f denotes frequency.

Figure 6.- Continued.

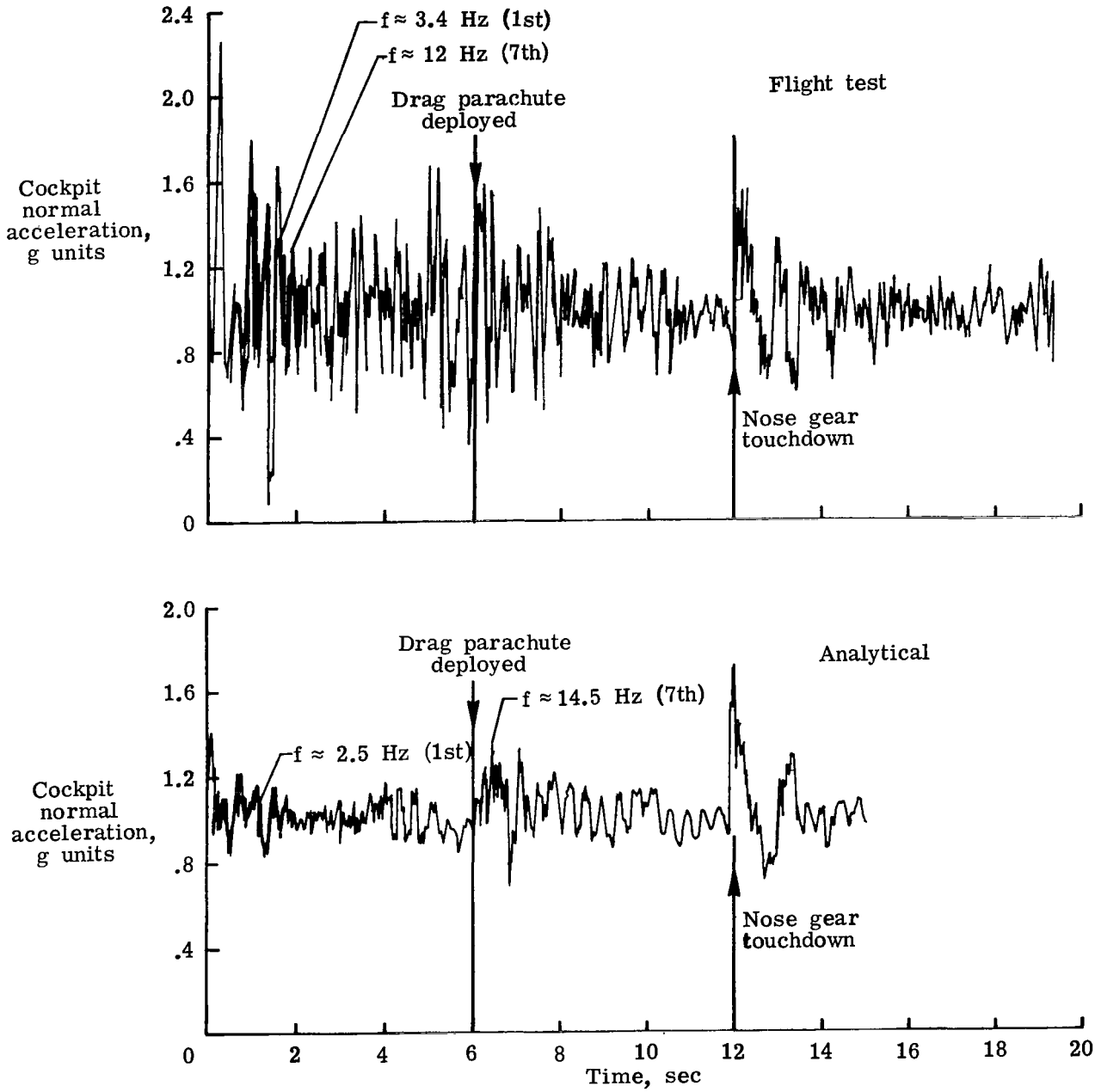

(o) Normal acceleration of cockpit. f denotes frequency.

Figure 6.- Continued.

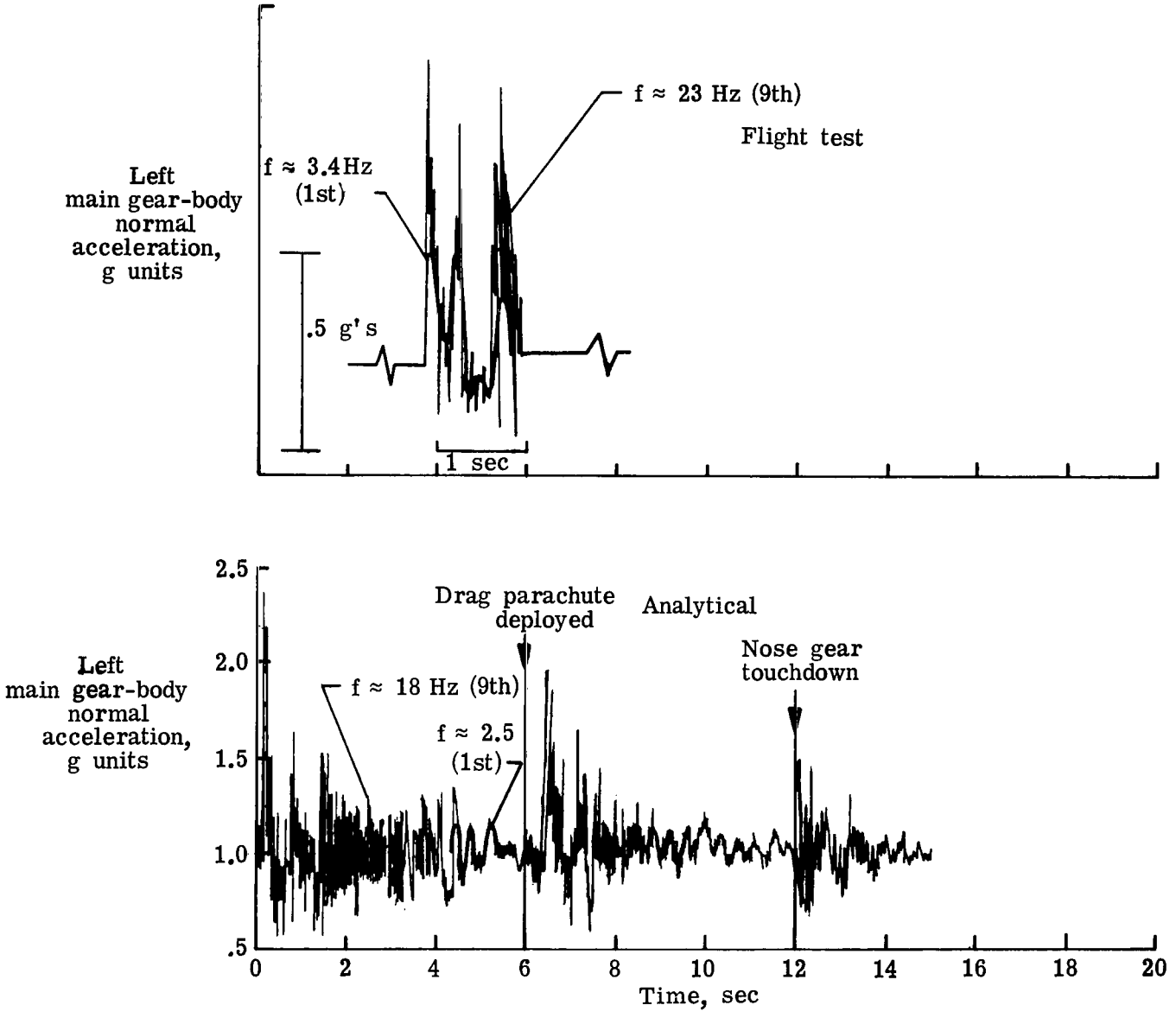

(p) Normal acceleration of left main gear body. f denotes frequency.

Figure 6.- Concluded.

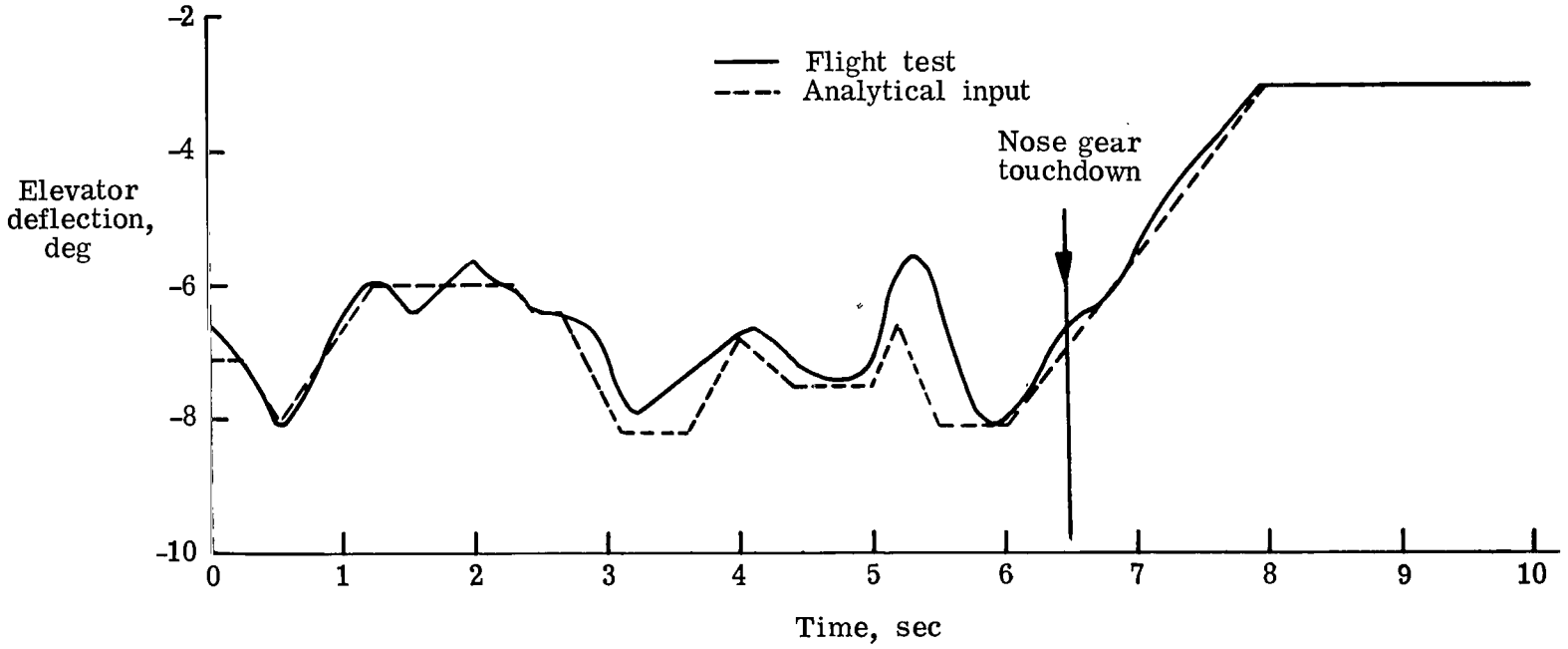

(a) Elevator deflection.

Figure 7.- Analytical flexible-body and flight test data for asymmetric touchdown of YF-12A airplane.

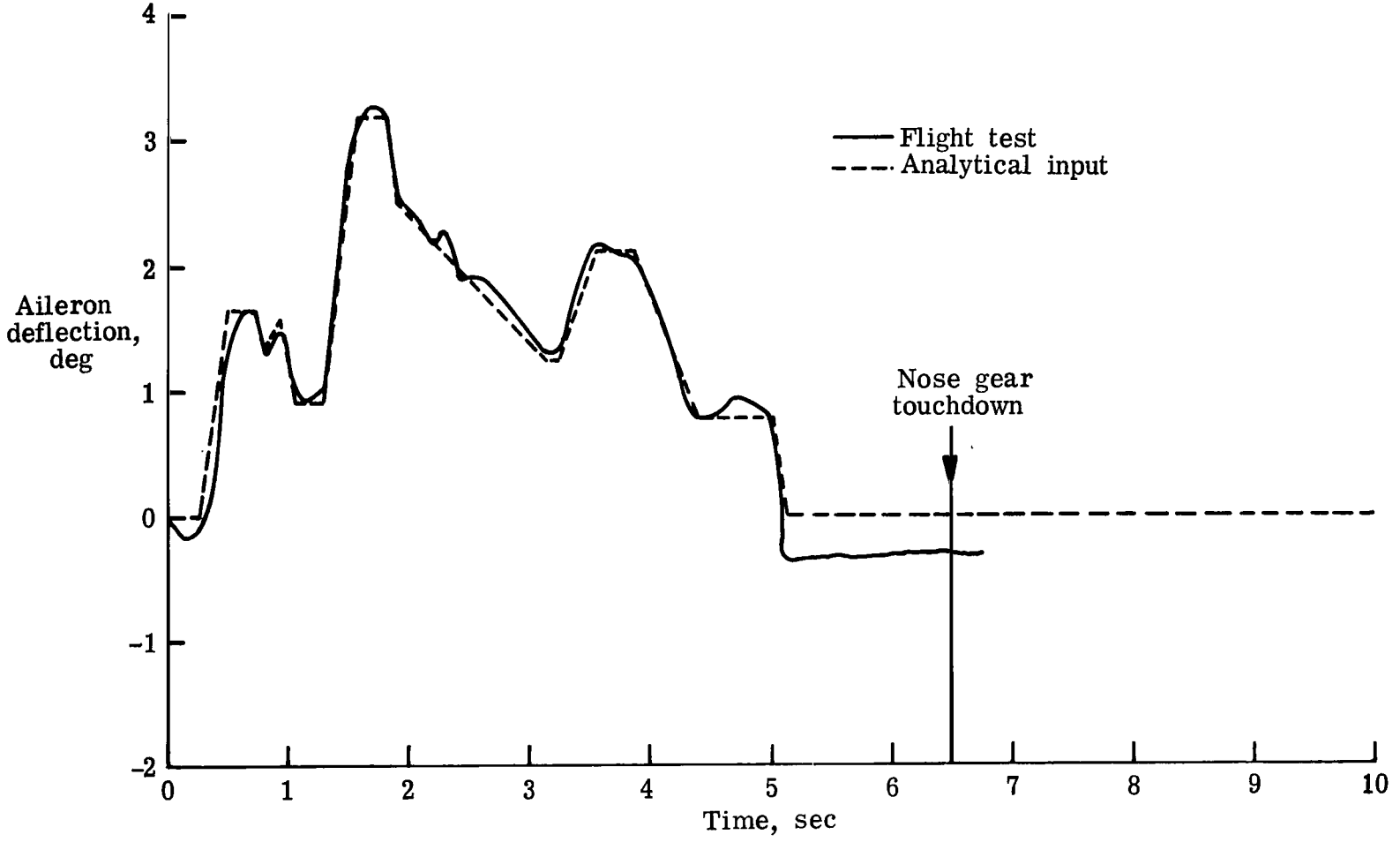

(b) Aileron deflection.

Figure 7.- Continued.

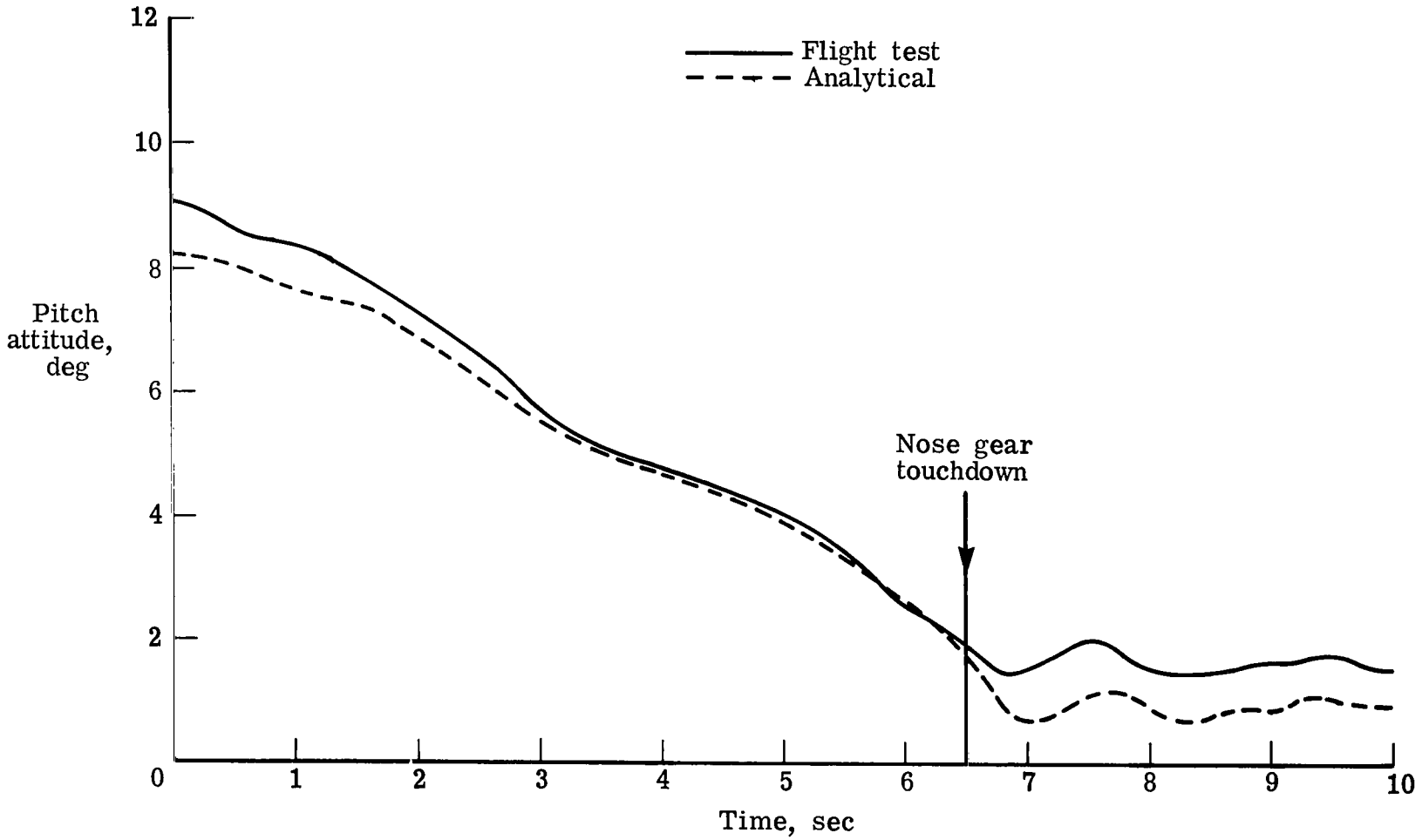

(c) Pitch attitude.

Figure 7.- Continued.

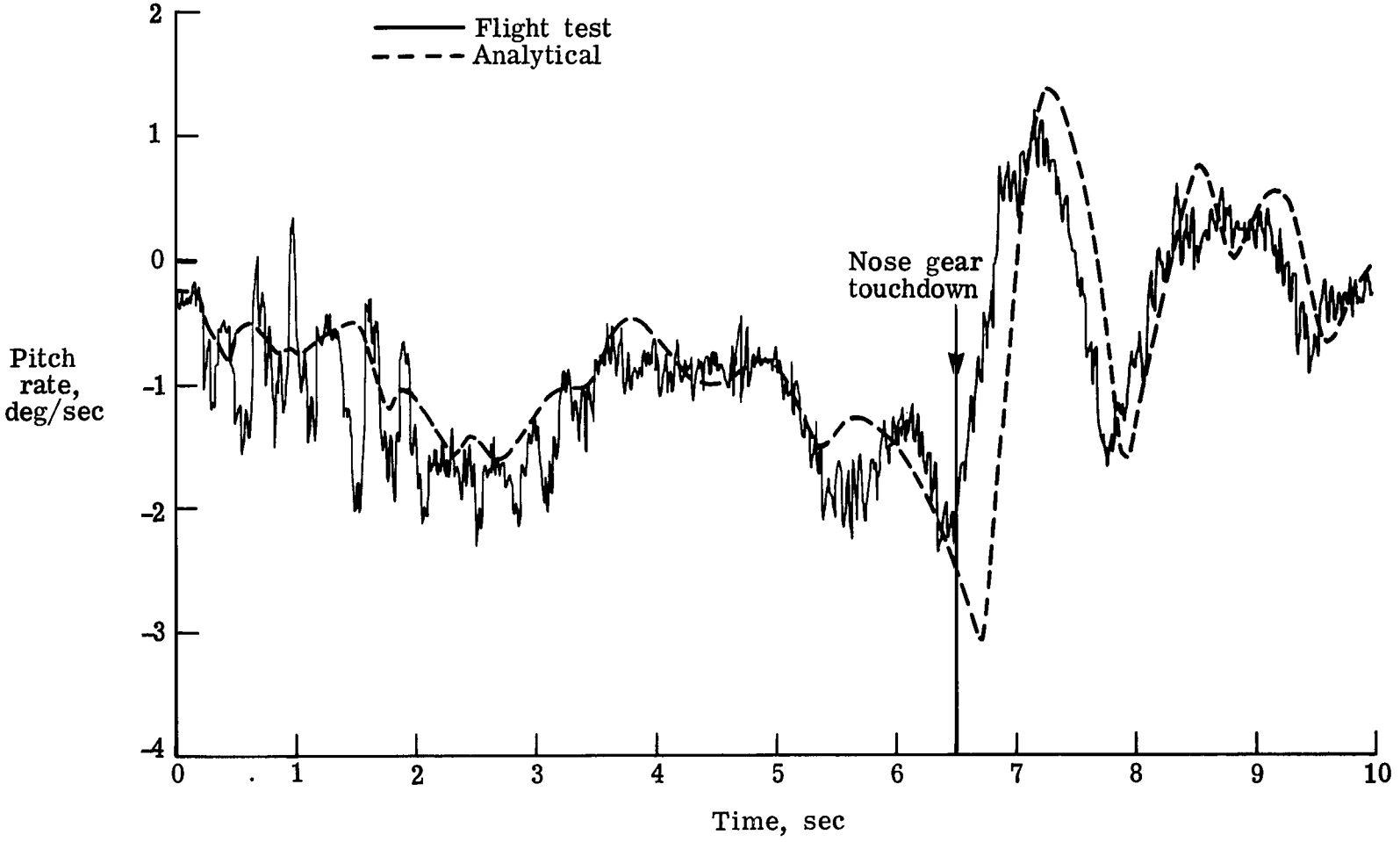

(d) Pitch rate.

Figure 7.- Continued.

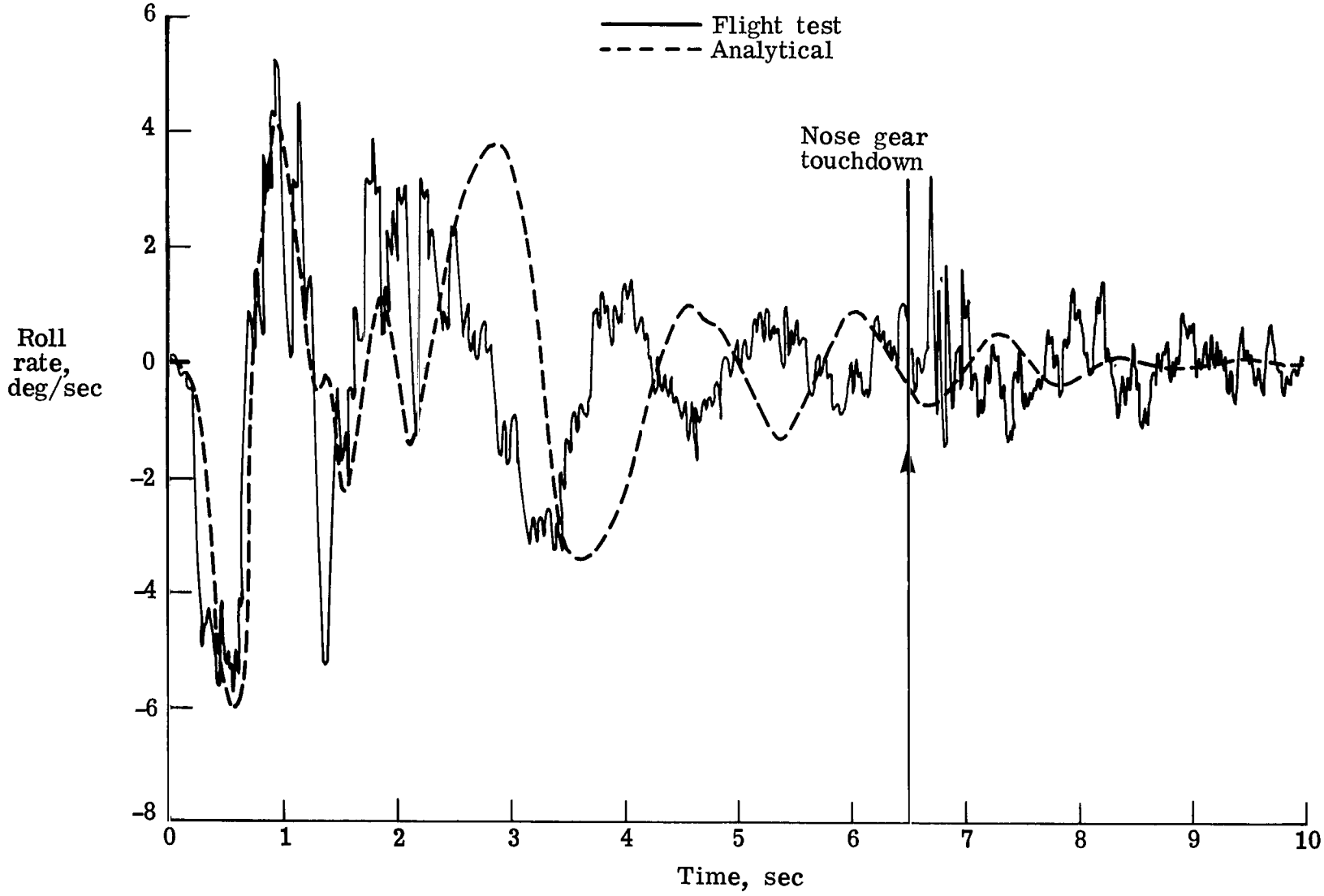

(e) Roll rate.

Figure 7.- Continued.

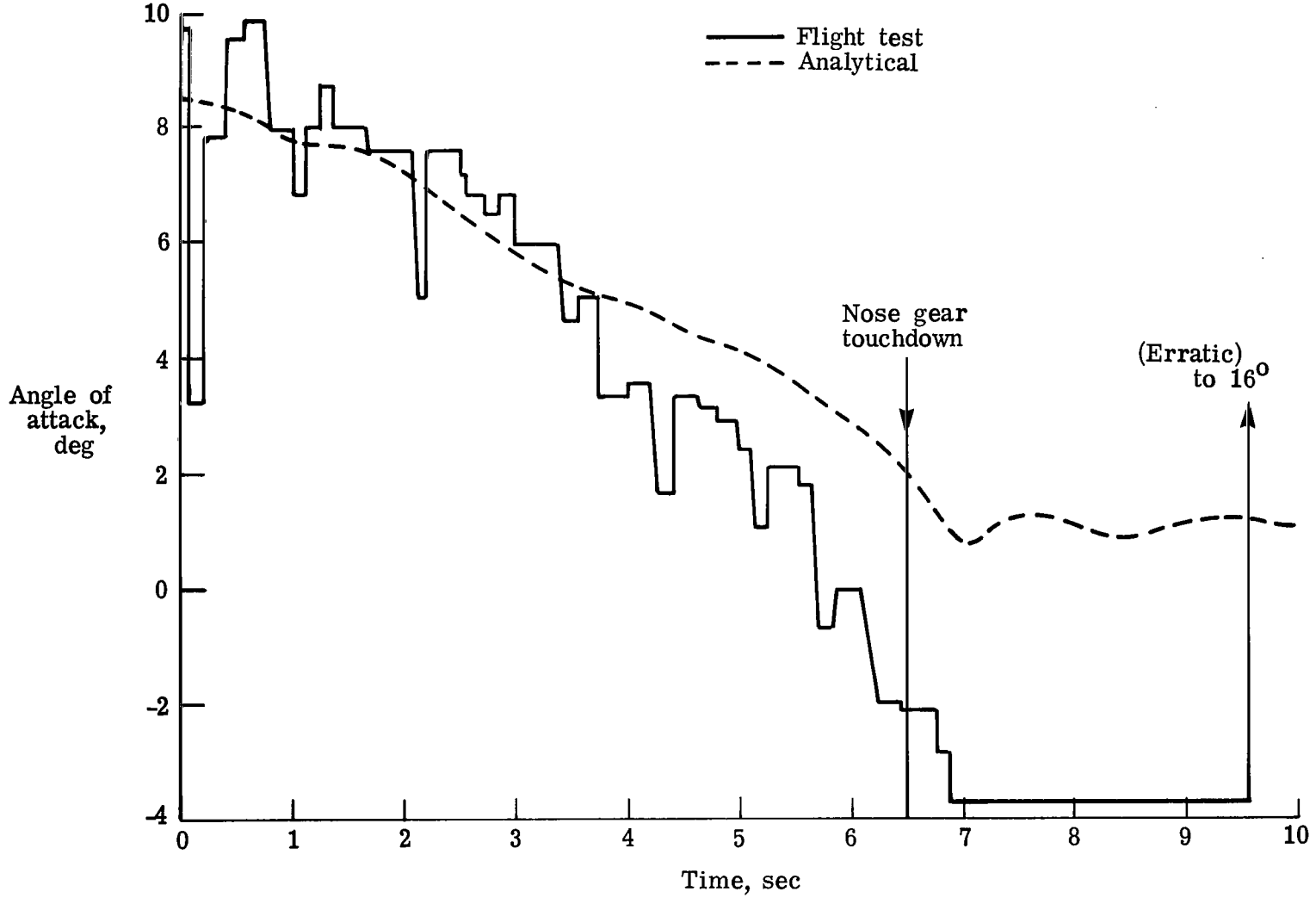

(f) Angle of attack.

Figure 7.- Continued.

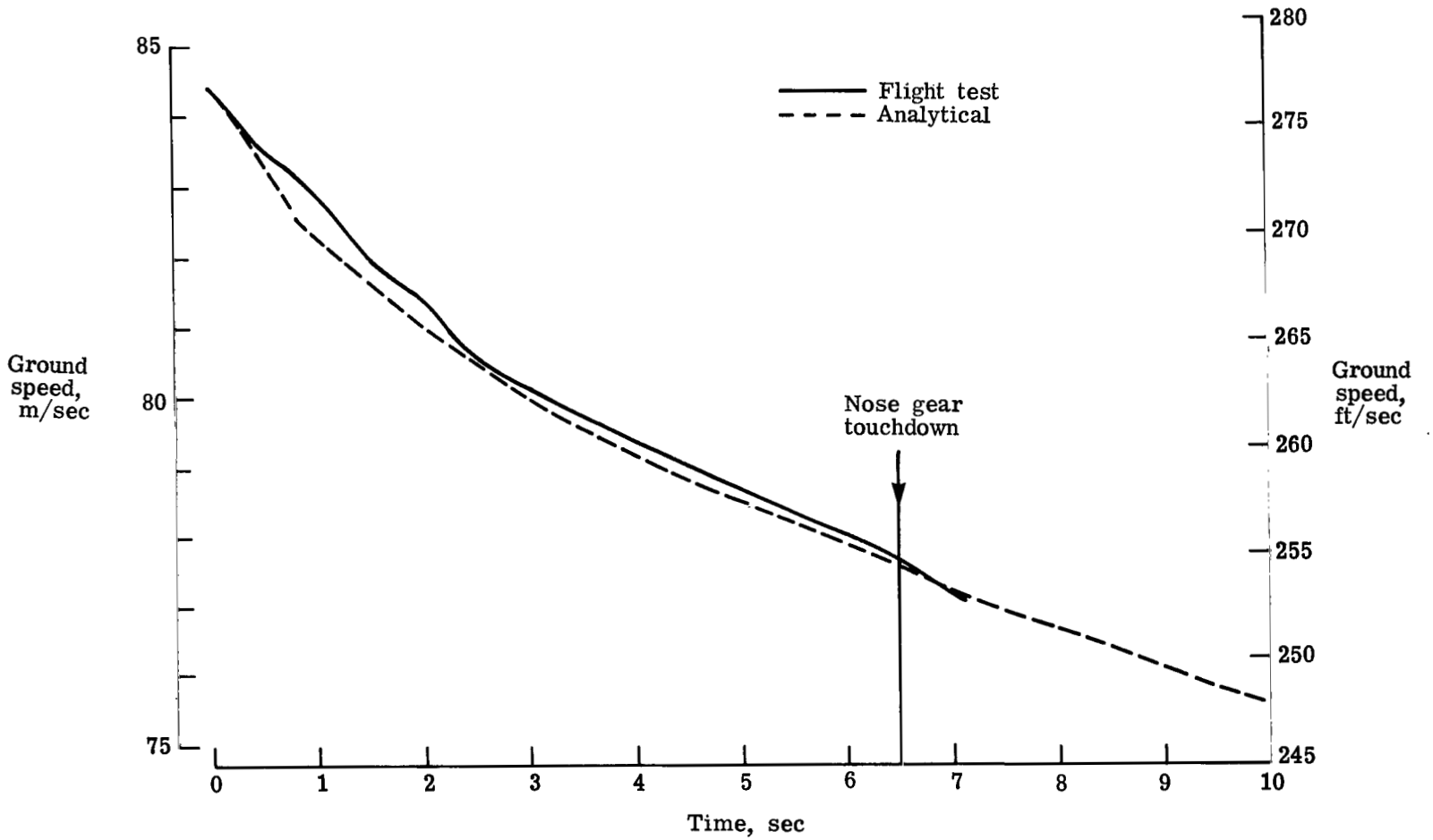

(g) Ground speed.

Figure 7.- Continued.

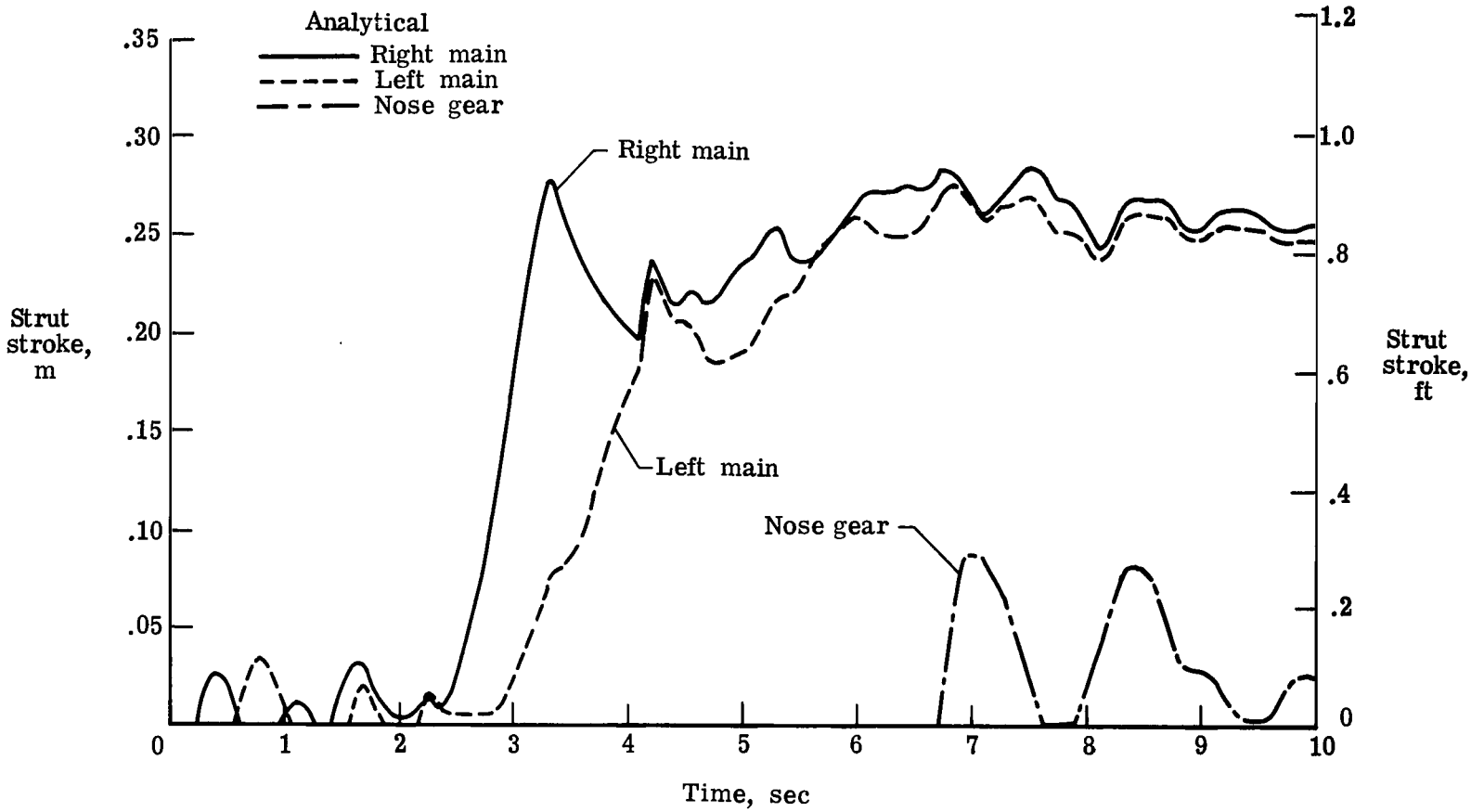

(h) Strut strokes.

Figure 7.- Continued.

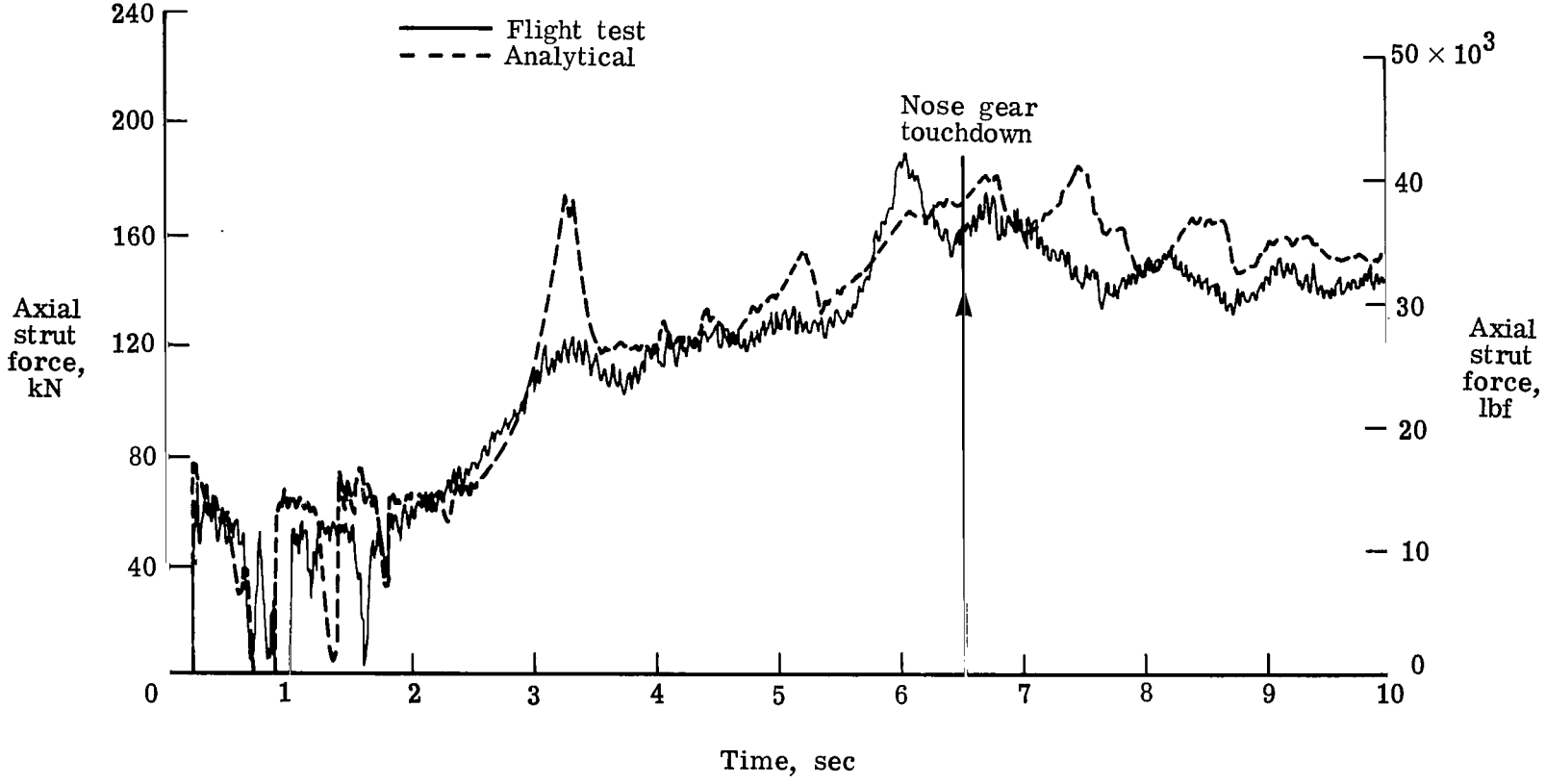

(i) Right main gear axial strut force.

Figure 7.- Continued.

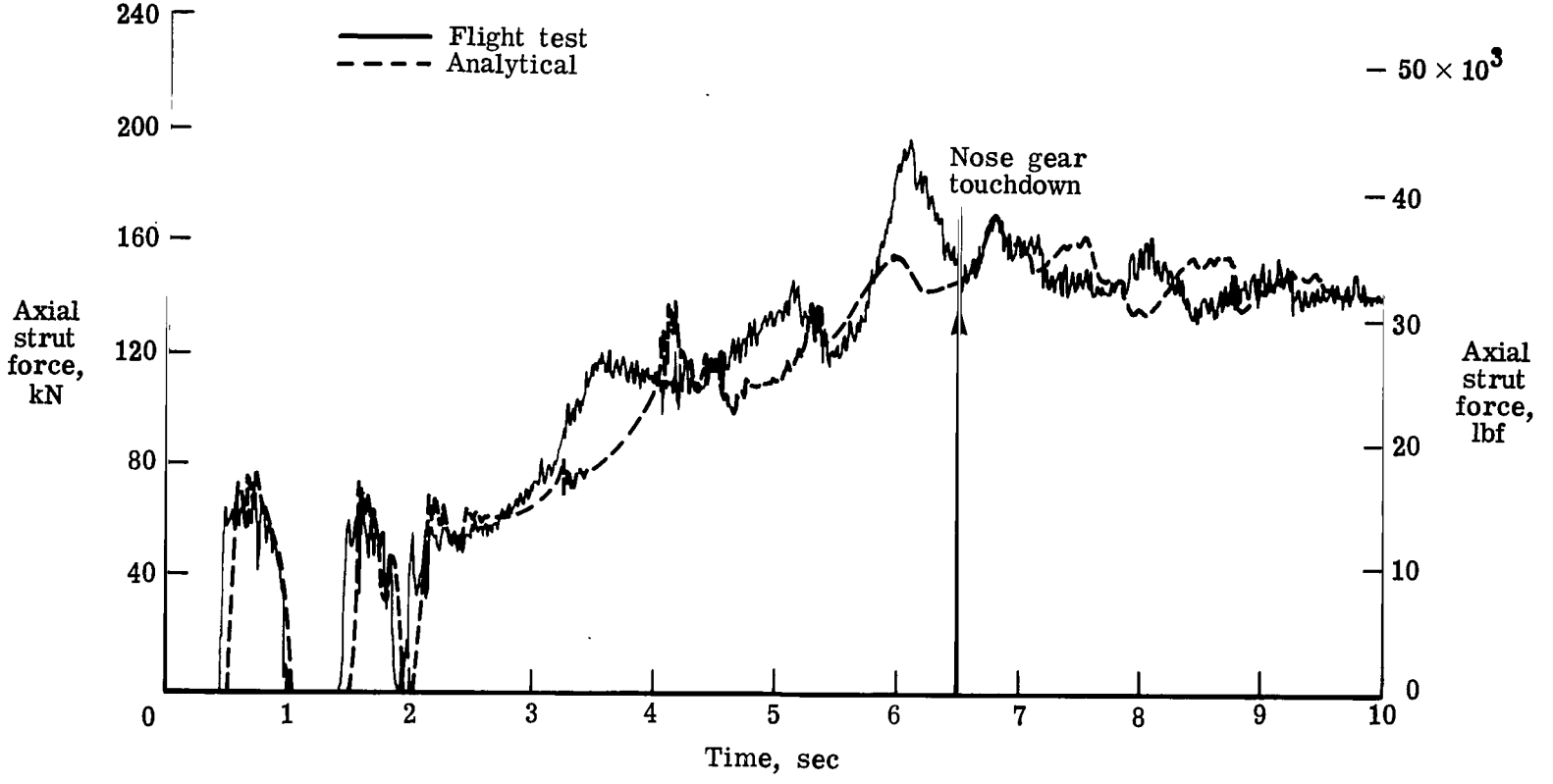

(j) Left main gear axial strut force.

Figure 7.- Continued.

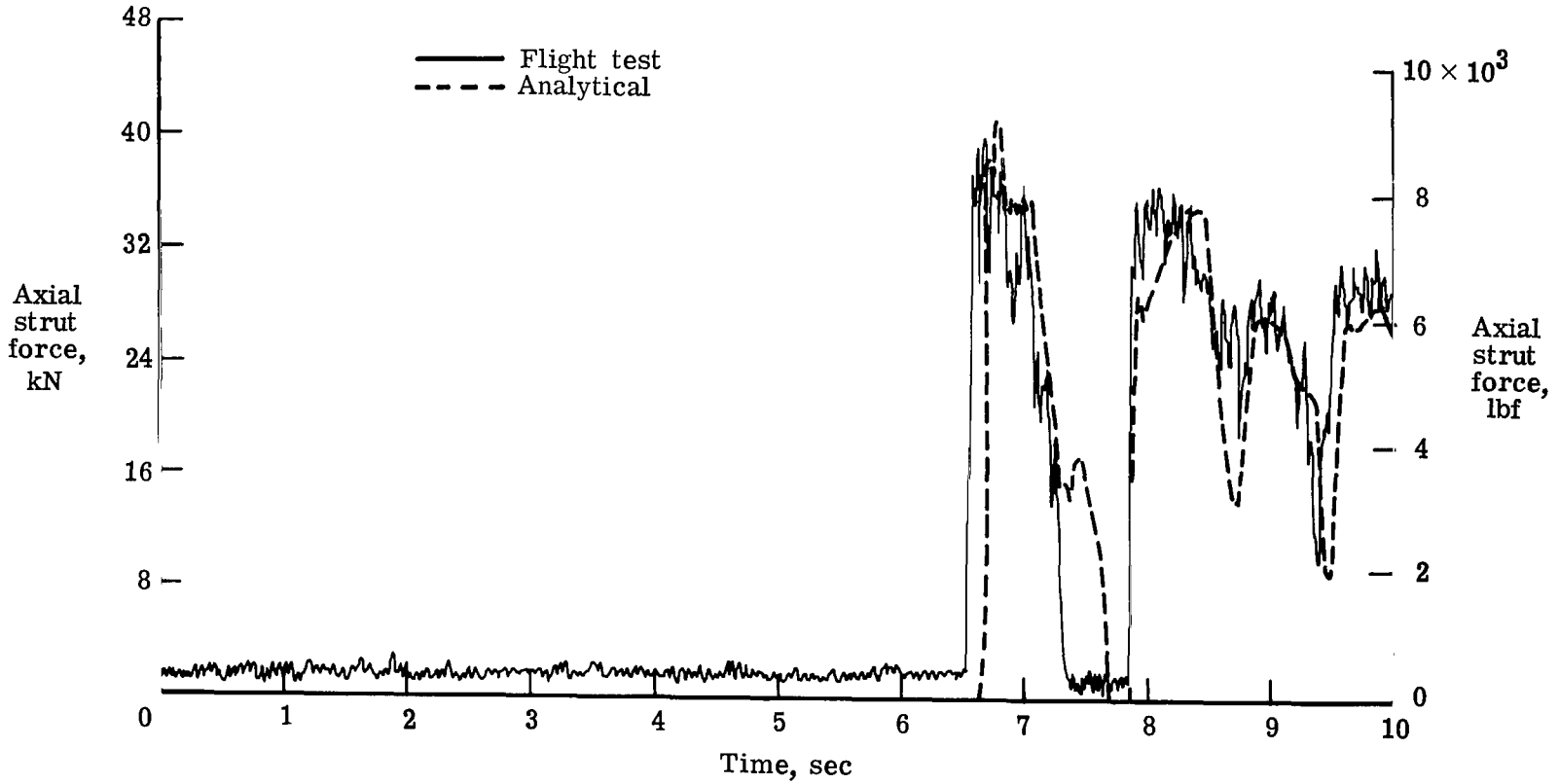

(k) Nose gear axial strut force.

Figure 7.- Continued.

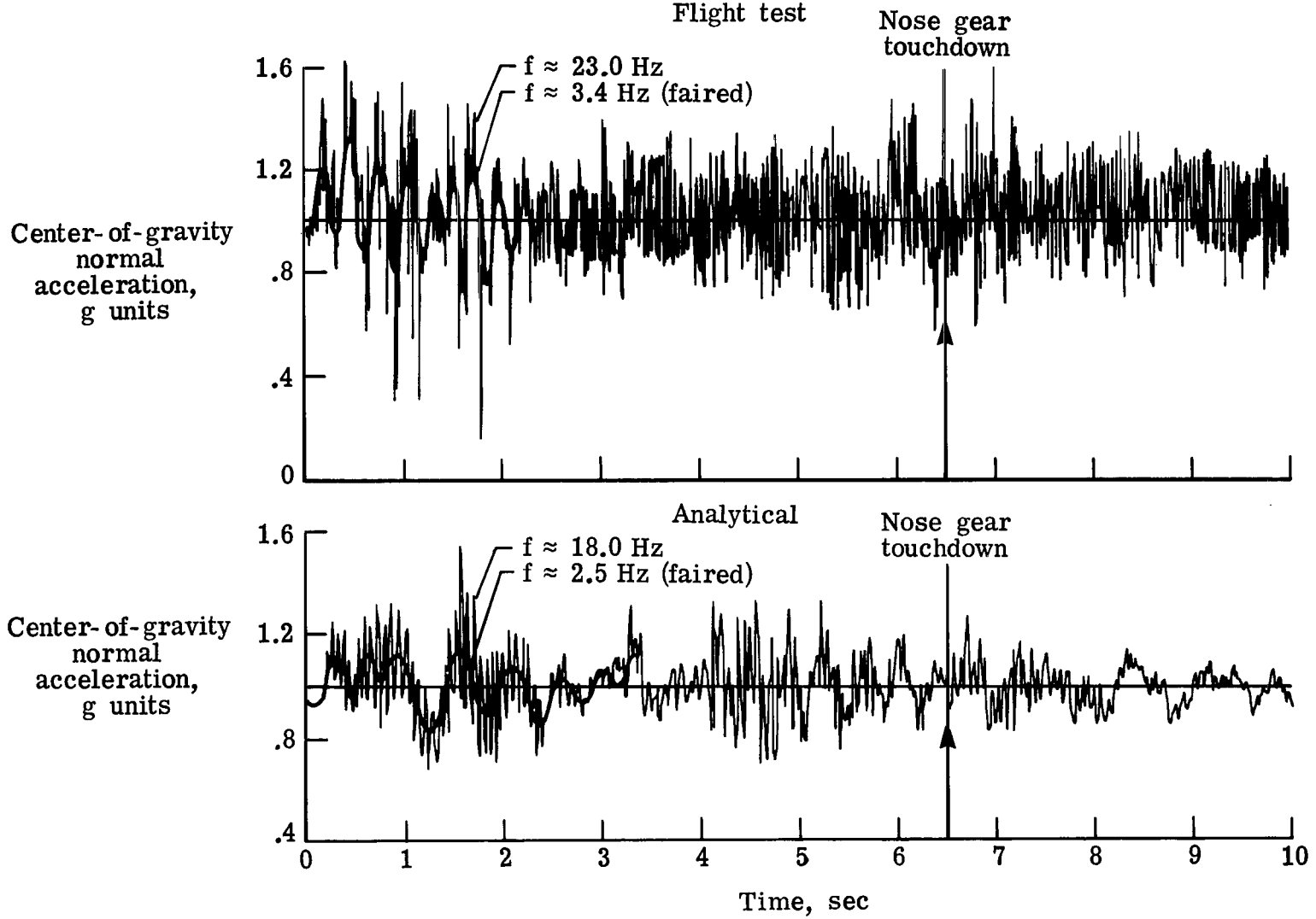

(1) Normal acceleration of center of gravity. f denotes frequency.

Figure 7.- Continued.

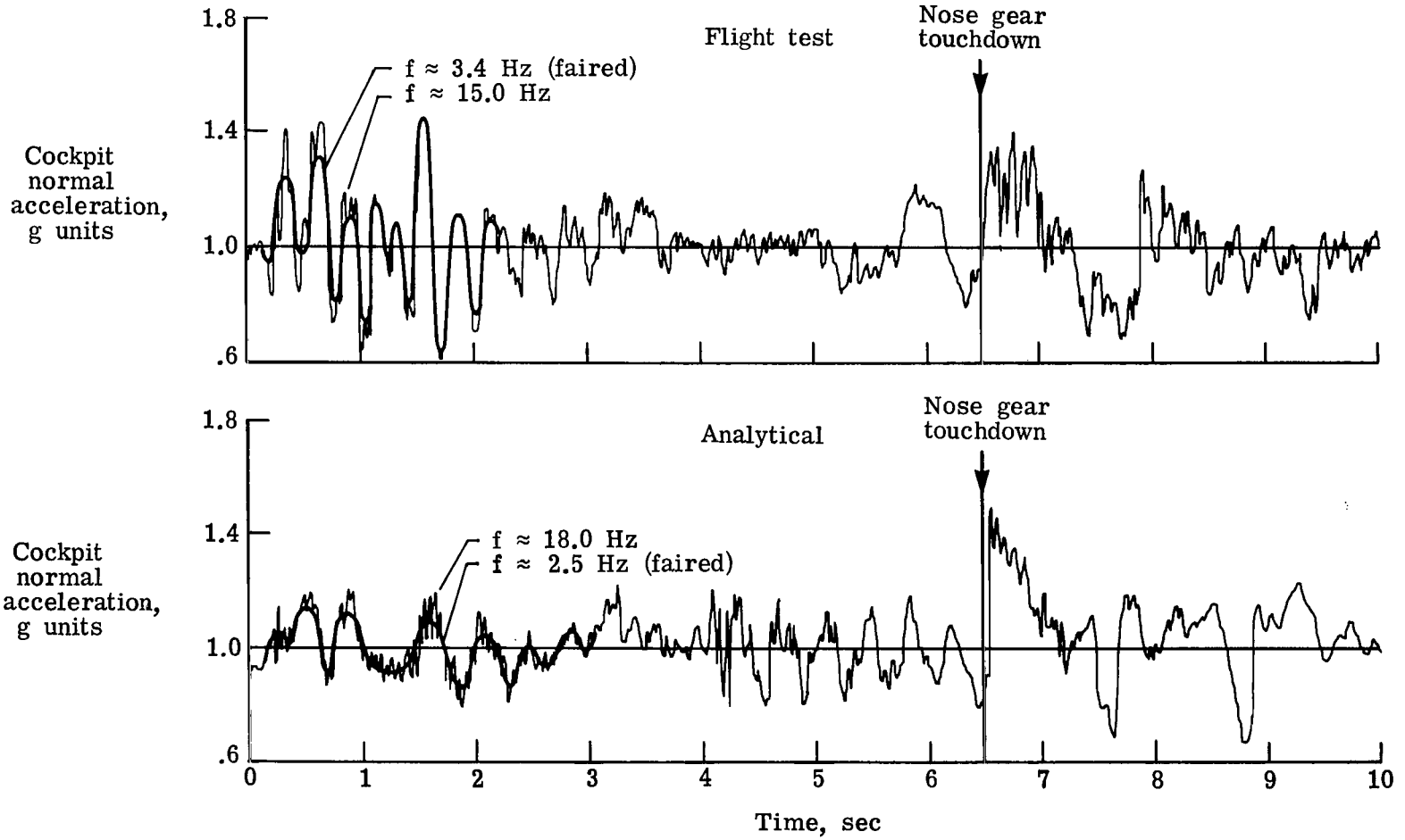

(m) Normal acceleration of cockpit. f denotes frequency.

Figure 7.- Continued.

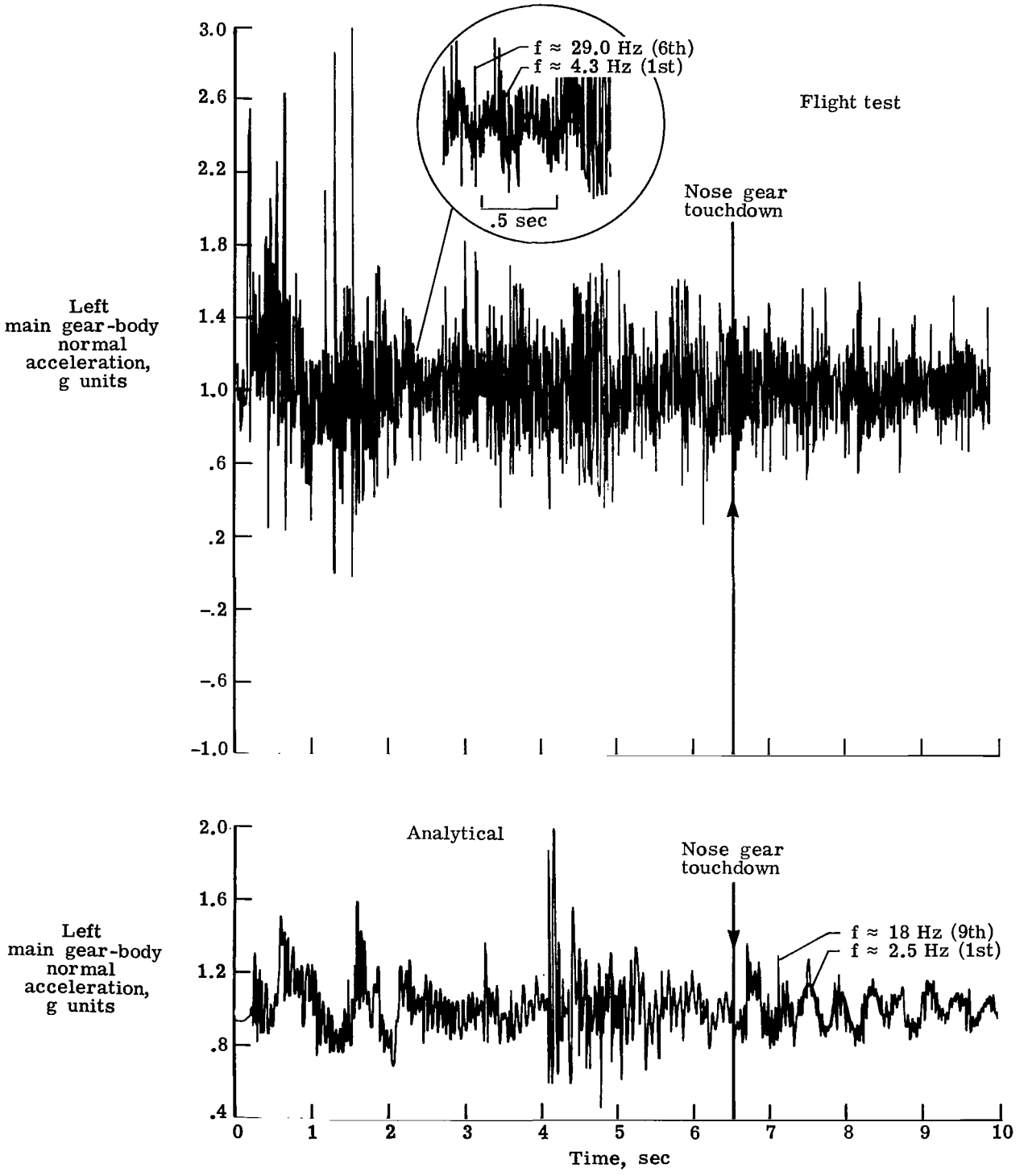

(n) Normal acceleration of left main gear-body interface.

Figure 7.- Concluded.

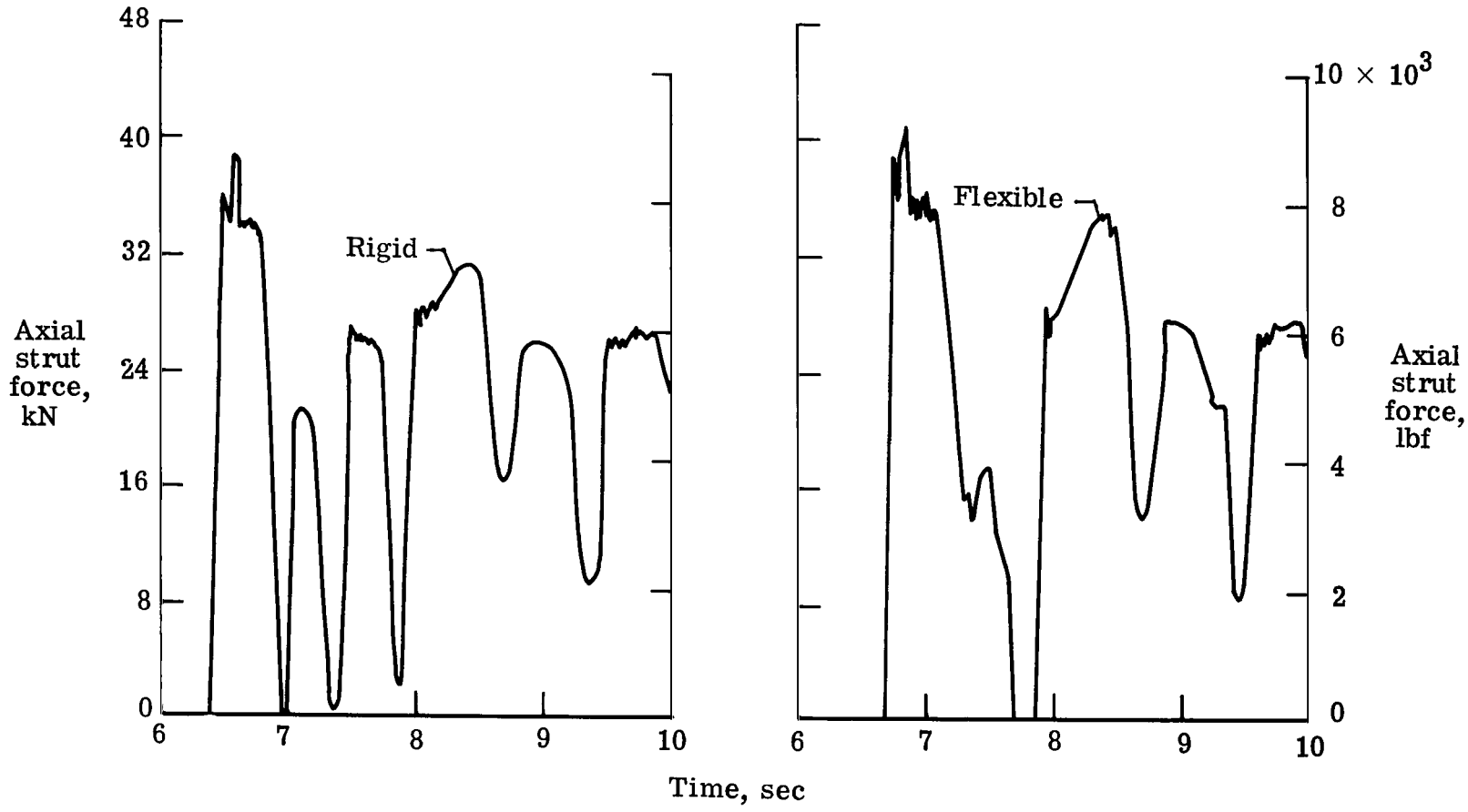

Figure 8.- Analytical rigid-body and flexible-body nose gear axial strut forces for YF-12A airplane.

1. Report No.	2. Government Accession No.	3. Recipient's Catalog No.
NASA TP-1025		

4. Title and Subtitle	5. Report Date
VALIDATION OF A FLEXIBLE AIRCRAFT TAKE-OFF AND LANDING ANALYSIS (FATOLA)	October 1977
	6. Performing Organization Code
7. Author(s)	8. Performing Organization Report No.
Huey D. Carden and John R. McGehee	L-11704
	10. Work Unit No. 743-01-12-03
9. Performing Organization Name and Address NASA Langley Research Center Hampton, VA 23665	11. Contract or Grant No.
	13. Type of Report and Period Covered Technical Paper
12. Sponsoring Agency Name and Address National Aeronautics and Space Administration Washington, DC 20546	14. Sponsoring Agency Code

15. Supplementary Notes

16. Abstract

Modifications to improve the analytical simulation capabilities of a multi-degree-of-freedom Flexible Aircraft Take-off and Landing Analysis (FATOLA) computer program are discussed. The FATOLA program was used to simulate the landing behavior of a stiff-body X-24B reentry research vehicle and of a flexible-body supersonic cruise YF-12A research airplane. The analytical results were compared with flight test data, and correlations of vehicle motions, attitudes, forces, and accelerations during the landing impact and rollout were good. For the YF-12A airplane, airframe flexibility was found to be important for nose gear loading. Based upon the correlation study presented herein, the versatility and validity of the FATOLA program for the study of landing dynamics of aircraft are confirmed.

17. Key Words (Suggested by Author(s))	18. Distribution Statement
Flexible aircraft Landing behavior Landing analysis Aircraft response	Unclassified - Unlimited Subject Category 05

19. Security Classif. (of this report)	20. Security Classif. (of this page)	21. No. of Pages	22. Price*
Unclassified	Unclassified	66	$4.50

* For sale by the National Technical Information Service, Springfield, Virginia 22161

NASA-Langley, 1977